BIOINFORMATICS

Vol. 00 no. 00 2015
Pages 1–8

SplAdder: Identification, quantification and testing of alternative splicing events from RNA-Seq data

André Kahles,[1,*] Cheng Soon Ong,[2] Yi Zhong,[1] and Gunnar Rätsch[1,*]

[1]Memorial Sloan Kettering Cancer Center, 1275 York Avenue, New York, NY 10065, USA
[2]NICTA, Canberra Research Laboratory, Tower A, 7 London Circuit, Canberra ACT 2601, Australia

Received on XXXXX; revised on XXXXX; accepted on XXXXX

Associate Editor: XXXXXXX

ABSTRACT

Motivation: Understanding the occurrence and regulation of alternative splicing (AS) is a key task towards explaining the regulatory processes that shape the complex transcriptomes of higher eukaryotes. With the advent of high-throughput sequencing of RNA (RNA-Seq), the diversity of AS transcripts could be measured at an unprecedented depth. Although the catalog of known AS events has grown ever since, novel transcripts are commonly observed when working with less well annotated organisms, in the context of disease, or within large populations. Whereas an identification of complete transcripts is technically challenging and computationally expensive, focusing on single splicing events as a proxy for transcriptome characteristics is fruitful and sufficient for a wide range of analyses.

Results: We present *SplAdder*, an alternative splicing toolbox, that takes RNA-Seq alignments and an annotation file as input to *i)* augment the annotation based on RNA-Seq evidence, *ii)* identify alternative splicing events present in the augmented annotation graph, *iii)* quantify and confirm these events based on the RNA-Seq data, and *iv)* test for significant quantitative differences between samples. Thereby, our main focus lies on performance, accuracy and usability.

Availability: Source code and documentation are available for download at `http://github.com/ratschlab/spladder`. Example data, introductory information and a small tutorial are accessible via `http://bioweb.me/spladder`.

Contact: andre.kahles@ratschlab.org, gunnar.ratsch@ratschlab.org

1 INTRODUCTION

Alternative splicing (AS) is an mRNA processing mechanism that cuts and re-joins maturing mRNA in a highly regulated manner, thereby increasing transcriptome complexity. Depending on the organism, up to 95% of expressed genes are transcribed into multiple transcript variants (Pan *et al.*, 2008; Wang *et al.*, 2008), where various transcripts with differing exon composition can arise from the same gene locus. (Throughout this text, we will use the term *transcript* to identify a variant of a gene that was generated through transcriptional processing.) Although these transcripts might never coexist at the same time and place, each one of them can be essential for cell differentiation, development or play an important role within signaling processes (Kornblihtt *et al.*, 2013). Thus, the two major challenges in computational transcriptome analysis are complexity and completeness. In *SplAdder*, we leverage evidence from RNA-Seq data to compute a more complete representation of the splicing diversity within a sample and tackle the complexity with a reduction to alternative splicing events instead of full transcripts. We provide open source implementations for *SplAdder* in MATLAB and Python that contain all features described below and produce the same results. However, future development will focus on the Python implementation for reasons of accessibility. All inputs follow the standardized formats for alignments and annotation such as BAM and GFF. For complete examples, use cases and information regarding the user interface, we provide a supplementary website. User documentation is available in the wiki section of the source code repository.

In Section 2 we will give a brief overview on related approaches that also focus on the analysis and quantification of alternative splicing based on RNA-Seq data. Our main focus will be on methods that are able to characterize alternative splicing events. In the subsequent Section 3, we give an outline of the *SplAdder* methodology and the algorithmic details of its main compute phases. To show how *SplAdder* compares to other strategies for RNA-Seq based alternative splicing analysis, we have compiled a set of different evaluations and comparisons to existing methods. Our experimental design will be described in Section 4 and the main results are discussed in Section 5. Lastly, Section 6 summarizes this work.

2 RELATED WORK

Prior to the advent of high throughput RNA-Seq, methods based on expressed sequence tags (ESTs) were developed to elucidate the complex patterns of alternative splicing in higher organisms (Modrek and Lee, 2002). Although designed for a much lower data throughput, the algorithmic ideas presented for ESTs have had a strong influence to the field in the following years. One central idea is the representation of splicing variation at a gene locus as a graph that encodes exon segments as nodes and the intron segments as connecting edges (Heber *et al.*, 2002; Eichner *et al.*, 2011; Kianianmomeni *et al.*, 2014). Similar to *SplAdder*, numerous tools are based on such splicing graph representations; however, none of the existing approaches combines all aspects of the *SplAdder* workflow: the augmentation of existing annotation information, the detection and quantification of alternative splicing events, differential testing of events between two given sets of

*to whom correspondence should be addressed

samples and detailed visualization of the splicing variation. There exist several approaches that cover at least a subset of the steps in the *SplAdder* pipeline. The most notable ones are *JuncBase* (Brooks *et al.*, 2011), *rMATS* (Shen *et al.*, 2014) and *SpliceGrapher* (Rogers *et al.*, 2012). *JuncBase* utilizes third party prediction tools such as *Cufflinks* (Trapnell *et al.*, 2010) to allow for the detection of novel exon nodes in the splicing graph. It then extracts and quantifies splicing events of the most common AS types and reports them in a custom format. Further, *JuncBase* provides basic differential analyses and basic visualizations of the test results. However, the pipeline consists of 10 different steps, including building a *Cufflinks* output based database, which is quite laborious to generate, has a long running-time and is thus not ideal for larger scale studies. *SpliceGrapher* directly integrates information from RNA-Seq or EST data into a splicing graph and can display splicing events in the graph visualizations. Unfortunately, it does not provide an easy method to explicitly generate and quantify alternative splicing events and does not allow for differential analysis. *rMATs* focuses on the differential analysis of splicing between RNA-Seq samples. It can detect the most common AS events from either RNA-Seq alignments or from a set of reads by applying a third party mapping algorithm. Based on the RNA-Seq evidence, it will also fill in some missing information to call events not present in the provided annotation but has a limited capacity to do so.

Other methods, such as *Scripture* (Guttman *et al.*, 2010), *Cufflinks* (Trapnell *et al.*, 2010) or *MISO* (Katz *et al.*, 2010) also use graphs internally and allow for novel splice variants based on RNA-Seq evidence but focus on the prediction of full transcripts instead of single events. These tools aim to solve a much harder problem and thereby miss potential local variability for AS studies. These tools are also computationally more expensive, limiting their applicability in the context of thousands of samples. Another popular tool that is focused on the extraction of alternative splicing events from a given annotated locus is the *Astalavista* toolbox (Foissac and Sammeth, 2007). Although many splicing events are covered in the detection phase, the tool relies on a complete annotation as input and does not provide any quantification values for the events However, the authors introduce a logical representation of splice events (the splicing code) that we will utilize later on. The software *SpliceTrap* (Wu *et al.*, 2011) is able to generate quantification values for the most common AS types, but recognizes much fewer transcripts than *Astalavista*. For both tools no novel splice variants are considered.

In our evaluation on simulated data, we will show that *SplAdder* is more accurate in detecting novel events and shows better performance in differential analysis than any of the tested competitors. We have chosen to compare *SplAdder* against *JuncBase*, *rMATS* and *SpliceGrapher* as these methods are closest to the presented *SplAdder* pipeline. We discuss further details regarding the comparisons in Section 4 and Suppl. Section D.

3 APPROACH

The *SplAdder* algorithm consists of multiple steps that convert a given annotation into a splicing graph, enrich that graph with splicing evidence from RNA-Seq samples, identify splicing events from the augmented graph and use the given RNA-Seq data to quantify the single events (Figure 1). Optionally, the quantifications can then be used for differential analysis. We find this distinction important, as differential analysis between samples is only one of many possible applications of AS event phenotypes. Other examples may include generating of sample specific splicing profiles or using AS phenotypes in genome-wide association studies.

3.1 Preliminaries

Here, we will introduce our notation and make definitions that will be used throughout the following descriptions of the algorithm.

Coordinates All positions used in the following descriptions are in a genomic coordinate system. We begin by defining the genome $\mathbb{G}$ as a string of consecutive positions $\mathbb{G} = g_1 g_2 \dots g_n$. When addressing any range x within these positions, e.g., to define a gene x, we describe this as the pair of the first and the last position of $x : (g_{x,\text{start}}, g_{x,\text{end}})$. When addressing a specific entity x_i, we will write $(g_{x_i,\text{start}}, g_{x_i,\text{end}})$. For simplicity, we ignore chromosomes and assume the genome to be one continuous string.

Representation of Genes as Transcript Graphs A given gene annotation can be represented as a set of linear directed graphs. Assume gene $\mathcal{G}$ as given, that has k different transcripts $j_1, \dots, j_k \in J_\mathcal{G}$, where $J_\mathcal{G}$ is the set of all transcripts of gene $\mathcal{G}$. As we consider each gene $\mathcal{G}$ independently, we will omit the index $\mathcal{G}$ wherever possible in order to keep the notation uncluttered. Each transcript consists of a set of exons that are connected by introns. Each exon can be uniquely identified by its start and end. We thus represent all exons as coordinate pairs of their genomic start and end position:

$$v = (\text{start}, \text{end}) = (g_{v,\text{start}}, g_{v,\text{end}}) \in \mathbb{N}^2,$$

where $g_{v,\text{start}}$ and $g_{v,\text{end}}$ are the first and last position of exon v in genomic coordinates, respectively. Although further coordinate information like chromosome and strand are used in the program implementation, we will limit this description to an identification by start and end for simplicity. The exons of each transcript j_i can then be represented as a node set $V_i := \{v_{i,1}, \dots, v_{i,m_i}\}$ with $1 \leq i \leq k$ and m_i as the number of exons in transcript j_i. As transcripts have a direction (the exons within a transcript follow a strict order), we require, that the index of the nodes reflects the order of the exons in the transcript. As no two exons in a transcript overlap by definition, this order is implied by $g_{v,\text{start}}$ and $g_{v,\text{end}}$. We then define the edge set of transcript j_i as

$$E_i := \bigcup_{1 \leq s < m_i} \{(v_{i,s}, v_{i,s+1}) \mid v_{i,s}, v_{i,s+1} \in V_i\} \subset V_i \times V_i$$

with $1 \leq i \leq k$. The pair (V_i, E_i) forms the directed *transcript graph* of transcript j_i.

Definition of Splicing Graphs We define the set of exons occurring in *any* transcript j_i as V. As the single exons are uniquely identified by their coordinates, we can write $V := \bigcup_{i=1}^{k} V_i$. Hence, we define the set of all edges as

$$E := \bigcup_{i=1}^{k} E_i \subset V \times V.$$

Note, that only already existing edges are merged, preserving the preexisting order of nodes. The pair $G = (V, E)$ is a directed acyclic graph and is called the *splicing graph* representation of a gene. Figure S-2 illustrates how a set of five transcripts is collapsed into a splicing graph. The key concept is, that when multiple transcripts contain the same exon, this will be represented by a single node in the splicing graph.

We define the *in-degree* and the *out-degree* of a node as the number of its incoming and outgoing edges, respectively. We further define a node to be *start-terminal*, if its in-degree is zero and *end-terminal* if its out-degree is zero. Each transcript can now be represented as a path through the splicing graph, beginning at a start-terminal node and ending at an end-terminal node.

Note, that although the splicing graph representation resolves many redundancies and efficiently stores large numbers of different but mostly overlapping transcripts, this comes at the cost of information loss. Long range dependencies between single exons are not preserved. An example

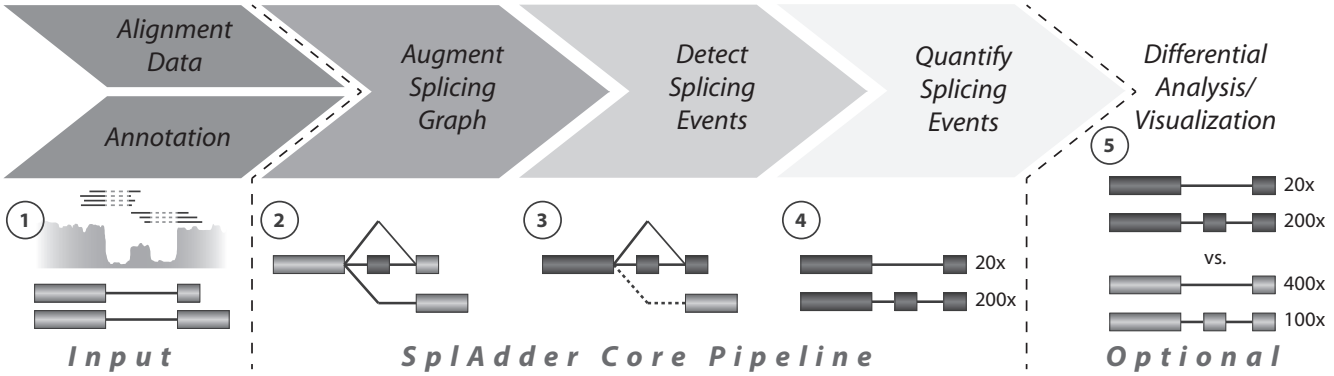

Fig. 1: ***SplAdder* Analysis Flowchart** The main steps of the *SplAdder* workflow consist of (1) integrating annotation information and RNA-Seq data, (2) generating an augmented splicing graph from the integrated data, (3) extraction of splicing events from that graph, (4) quantifying the extracted events, and optionally (5) the differential analysis between samples and producing visualizations.

of this is provided in Figure S-2. Although exon T2E1/T3E1 exclusively occurs in transcripts that end in exon T2E3/T3E3, this relationship is lost in the graph, where E2 can connect to both E6 and E7. Our approach is not severely affected by this limitation as we only extract local information about alternative exon- or intron-usage.

Definition of Segment Graphs Following the splicing graph definition, two or more nodes in the graph may overlap. Thus, when collecting expression information for each node from a given alignment, the same genomic positions may be queried multiple times. To overcome this inefficiency, we use the concept of breaking down each node into non-overlapping exon segments, similarly used in (Reyes *et al.*, 2012; Behr *et al.*, 2013).

The same principle that is applied when collapsing different transcripts that share the same exons into a graph structure can also be applied to collapse exon segments that are shared by several nodes of the splicing graph. Following this idea, we divide each exon into non-overlapping segments. Analogous to an exon, a segment is uniquely identified by its genomic coordinate pair and the same order as on exons can be applied: $s = (g_{s,\text{start}}, g_{s,\text{end}})$. We say an exon v_i is *composed* from segments $s_{i,q}$ through $s_{i,r}$, if $v_i = s_{i,q} \circ s_{i,r}$, with $q < r$ and where $\cdot \circ \cdot$ denotes the concatenation of segment positions. Thus, the set of all segments can be defined as

$$S = \bigcup_{v_i \in V} (s_{i,q}, \ldots, s_{i,r} \mid s_{i,q} \circ s_{i,r} = v_i).$$

To explicitly define the set of all segments, first we define the set V_S of all node-starts in V and the set V_T of all node ends in V. The set of all segments S can then be defined as

$$S = \bigcup_{g_{s,\text{start}}, g_{s,\text{end}} \in V_\text{TS}} \{(g_{s,\text{start}}, g_{s,\text{end}}) \mid \exists v \in V\colon g_{v,\text{start}} \leq g_{s,\text{start}} < g_{s,\text{end}} \leq g_{v,\text{end}}\},$$

where $V_\text{ST} = V_\text{S} \cup V_\text{T}$. The computation of S from V is straightforward. Let P be a sorted array containing all genomic positions that are either start or end positions of an exon in V. We denote the i-th element of the array as $P[i]$. Let L_S and L_E be two binary label-arrays with the same length as P, where $L_S[i]$ is 1 if $P[i]$ is start of an exon in V and 0 otherwise. Correspondingly, $L_E[i]$ is 1 if $P[i]$ is the end of an exon in V and 0 otherwise. Let further C_S and C_E be two arrays with the same length as P, where $C_S[i] = \sum_{j=1}^{i} L_S[i]$ and $C_E = \sum_{j=1}^{i} L_E[i]$ are the cumulative starts and ends up to position i. We can then determine the set of all segments as

$$S = \bigcup_{i=1}^{|P|-1} \{(P[i], P[i+1]) \mid C_S[i] > C_E[i]\}.$$

Similar to the definition of the edges for the splicing graph, we define

$$T = \bigcup_{s_u, s_w \in S} \{(s_u, s_w) \mid \exists v_i \in V, s_r \in S\colon v_i = (g_{s_r,\text{start}}, g_{s_u,\text{end}}) \text{ and } \exists v_j \in V, s_t \in S\colon v_j = (g_{s_w,\text{start}}, g_{s_t,\text{end}}) \text{ and } (v_i, v_j) \in E\}$$

to be the set of segment pairs that are connected by an intron. We then denote the pair $R = (S, T)$ to be the *segment* graph of a gene. For practical reasons, we store an additional matrix that relates each node in the splicing graph to the segments it is composed of. Supplemental Figure S-5 illustrates the relationship between splicing graph and segment graph.

We will use the splicing graph representation to incorporate new information based on RNA-Seq evidence as well as for the extraction of alternative splicing events. We will use the segment graph representation for event quantification, as this is computationally much more efficient.

3.2 Construction of an Augmented Splicing Graph

As a preprocessing step, the input annotation is transformed into the initial splicing graph G according to the definitions above, thereby collapsing exons shared by multiple transcripts into single nodes of the graph. In the following, we describe how G is transformed into an augmented graph $\hat{G}$ using information from RNA-Seq data, thereby introducing new nodes and edges. This is an integral part of the *SplAdder* workflow that enables the discovery of novel splicing variation based on RNA-Seq data.

The augmentation of G is a four-step algorithm:

1. build initial graph
2. add novel cassette exons
3. add novel intron retentions
4. while novel edges can be added
   4.1. insert novel intron edges

When a newly added node shares one boundary with an existing node, the existing edges are inherited by the new node. Following, we will provide a detailed explanation for each step.

Given an RNA-Seq sample and a gene $\mathcal{G} = (g_{\mathcal{G},\text{start}}, g_{\mathcal{G},\text{end}})$, we extract all intron junctions from the alignment that overlap $\mathcal{G}$ and show sufficient alignment support. Whether an intron junction is sufficiently well supported

is based on a set of given confidence criteria (cf. Supplemental Table C) We define the list of RNA-Seq intron junctions $\mathcal{R}$ as

$$\mathcal{R} = \{(g_i, g_j) \mid g_{\mathcal{G},\text{start}} \leq i < j \leq g_{\mathcal{G},\text{end}}\},$$

where (g_i, g_j) describes the intron starting at g_i and ending at g_j. Further, let $v = (g_{v,\text{start}}, g_{v,\text{end}})$, with $v \in V$, be an existing node in the splicing graph. The augmentation process will transform the existing splicing graph $G = (V, E)$ into an augmented graph $\hat{G} = (\hat{V}, \hat{E})$. We initialize $\hat{G}$ with G.

Adding Novel Cassette Exons In the first augmentation step, new cassette exon structures are added to the splicing graph. For this, the algorithm iterates over all non-overlapping pairs of $\mathcal{R}$. For each pair (g_{i_1}, g_{j_1}) and (g_{i_2}, g_{j_2}), two conditions need to be fulfilled. Briefly, both intron ends need to be attached to existing exons and the cassette exon must not already exist. Formally, we check for the following conditions:

Intron ends $\exists v_i \in \hat{V} : g_{v_i,\text{end}} = g_{i_1} - 1$
and $\exists v_j \in \hat{V} : g_{v_j,\text{start}} = g_{j_2} + 1$ and $v_i < v_j$

New exon $\nexists v_h \in \hat{V} : g_{v_h,\text{start}} = g_{j_1}$ and $g_{v_h,\text{end}} = g_{i_2}$.

If both conditions are met, a new node $v_n = (g_{j_1} + 1, g_{i_2} - 1)$ is added to the node set $\hat{V}$ and two new edges (v_i, v_n) and (v_n, v_j) are added to $\hat{E}$. Figure S-1, Panel A, schematically describes the addition of a cassette exon. The criteria for adding a cassette exon are listed in Supplemental Table A.

Adding Novel Intron Retentions The second augmentation step adds intron retention events to the splicing graph. For each edge $(v_s, v_t) \in \hat{E}$, the algorithm decides whether there is enough evidence from the given RNA-Seq sample for expression inside the intron, to consider the intron sequence as retained. Again, heuristic confidence criteria are applied (cf. Supplemental Table B). Briefly, the central criteria for adding a new intron retention is the number of sufficiently covered positions within the intron as well as the differences in mean coverage between intronic and exonic part of that region. When sufficient evidence for a retention is found, a new node $v_n = (v_{s,\text{start}}, v_{t,\text{end}})$ is added to $\hat{V}$. The new node inherits all incoming edges from v_s and all outgoing edges from v_t, thus we get the set of newly added edges

$$E_n = \left\{(x, v_n) \mid \forall x : (x, v_s) \in \hat{E}\right\} \cup \left\{(v_n, x) \mid \forall x : (v_t, x) \in \hat{E}\right\}.$$

Then, the set of edges is updated with $\hat{E} := \hat{E} \cup E_n$. Supplemental Figure S-1, Panel B, illustrates this case.

Insert Novel Intron Edges The last augmentation makes once more use of the list of RNA-Seq supported intron junctions $\mathcal{R}$ generated during the first step. Based on start and end position of the intron, we can test if any existing nodes start or end at these positions, respectively. We have to distinguish between four different basic cases: 1) neither start nor end coincide with any existing node boundary, 2) the intron-start coincides with an existing node end, 3) the intron end coincides with an existing node-start, 4) both the intron-start coincides with an existing node end and the intron-end coincides with an existing node-start. The four cases and their respective sub-cases are illustrated in Panels C–H of Supplemental Figure S-1. Formal definitions of the different cases are given in Supplemental Section A. As the addition of novel intron edges depends on other possibly novel edges, this addition step is repeated iteratively until no new edges can be added or a pre-defined maximum number of iterations is reached.

Splicing Graph Pruning When multiple RNA-Seq samples are available, *SplAdder* allows for an optional filtering step to reduce false positive edges. All edges that are not supported by a given minimum number of RNA-Seq samples will be pruned from the graph. Resulting orphan nodes that were not present in the initial graph will be pruned as well.

3.3 Detect and Quantify Alternative Splicing Events

Based on the augmented splicing graph, we extract various classes of AS events as subsets of connected nodes. *SplAdder* currently supports the following event types: exon skip, intron retention, alternative 3' and alternative 5' splice sites, multiple exon skips as well as mutually exclusive exons. Note, that currently alternative transcript starts and ends are not detected, as they are products of alternative transcriptional processing rather then results of alternative splicing. Each event is then represented as a "mini-gene" consisting of two splice variants minimally describing the alternatives of the event. Overlapping events that share the same intron coordinates and do only differ in the flanking exon ends are merged into a short common representation. We refer to Supplemental Section B.1 for the formal definitions of all classes of alternative events and a detailed description of the extraction algorithms.

Finally, the event set identified from the splicing graph is quantified using the given read alignment data. For each event, we report the mean coverage of each exon and the number of spliced alignments supporting each intron. Remember, that to speed up the quantification process, the read counting is performed on the segment graph representation defined above. Thus, no exon position needs to be quantified twice.

3.4 Differential Analysis

If the set of input samples can be separated into two or more groups representing different conditions, the splice quantifications produced by *SplAdder* can be subjected to differential testing. For this, *SplAdder* provides two basic strategies. The first is to use the *SplAdder* output files that describe event structure and quantification as input to other tools dedicated to analyze differential expression, such as *rDiff* (Drewe *et al.*, 2013) or DESeq (Reyes *et al.*, 2012). In previous studies, we have generally used the combination of *SplAdder* and *rDiff*. In this case, the mini genes predicted by *SplAdder* are re-quantified by *rDiff* and subjected to a test for differential relative transcript usage.

The second strategy is to directly use the exon-intron junction counts generated by *SplAdder* to apply a differential test. Briefly, we model junction read counts with a negative binomial distribution and employ a generalized linear model (GLM) framework for testing similar to (Love *et al.*, 2014). Similar to the previous approach, we use the sample replicate to estimate a mean variance relationship to better account for overdispersion. Details of the GLM based test is provided in Supplemental Section C. This strategy can be run as part of the *SplAdder* pipeline. It directly accesses the event quantifications and is computationally more efficient than the previous hybrid approach. We have included both strategies into our evaluation presented in Section 4.

3.5 Visualization

SplAdder also provides means for publication-ready visualization of the RNA-seq read coverage of exon positions and of intron junctions. Visualization allows for effective visual inspection of identified alternative splicing events in light of primary read data. These visualizations provide summarization of multiple samples as well as the comparison of different groups of samples to highlight differential splicing over several replicate groups or conditions. An example is provided in Supplemental Figure S-8.

4 EVALUATION AND APPLICATIONS

The *SplAdder* approach has been successfully applied in various biological studies on *Arabidopsis thaliana* (Drechsel *et al.*, 2013; Gan *et al.*, 2011) as well as in the context of large-scale cancer projects with several thousand RNA-seq libraries (Weinstein *et al.*, 2013). Here, we have created several sets of simulated data to evaluate *SplAdder*. Simulated data allows for an accurate measure of performance and provides a ground truth for a fair comparison against other existing methods. To allow as little bias

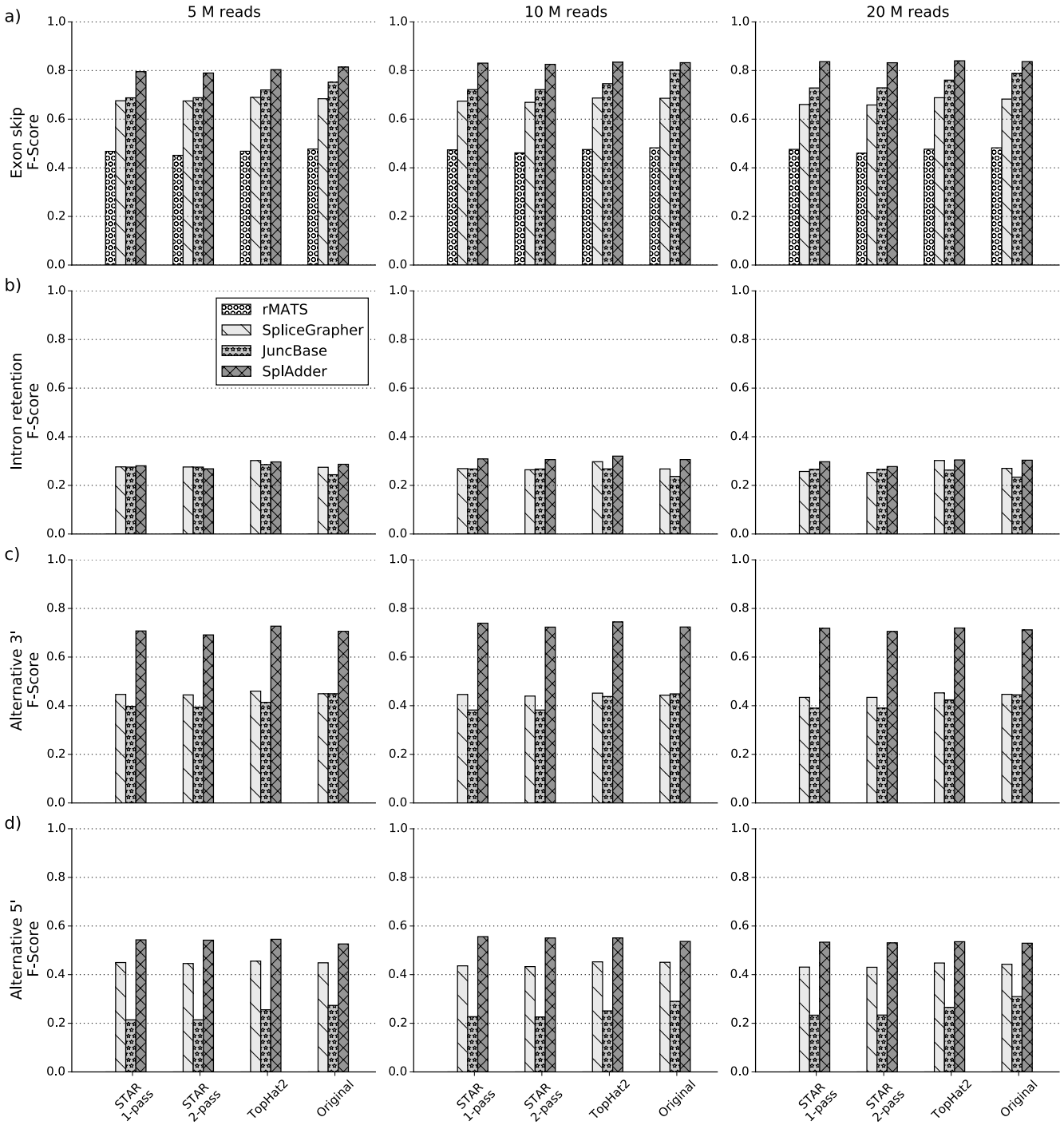

Fig. 2: ***SplAdder* Evaluation Results** This matrix of bar charts summarizes the evaluation results for the comparison of *rMATS*, *SpliceGrapher*, *JuncBase* and *SplAdder* (see legend) on different sets of simulated RNA-Seq read data. The metric shown here is the F-Score, defined as the harmonic mean of precision and recall. (Plots of the same design with details on precision and recall are provided in Supplemental Figures S-6 and S-7.) The rows of the plot matrix represent four different event types: a) exon skip, b) intron retention, c) alternative 3' splice site, and d) alternative 5' splice site. The columns represent different read set sizes (5 million, 10 million, 20 million). The four bar groups represent the different aligners used (from left to right: *STAR 1-pass*, *STAR 2-pass*, *TopHat2*, and the simulated ground truth alignment).

as possible towards our own method, we used an external data simulator (Griebel *et al.*, 2012). In the following, we describe the generated datasets and which evaluations were performed on them.

4.1 Data simulation

Detection of Novel Events We have used the *FluxSimulator* (Griebel *et al.*, 2012) toolbox to simulate RNA-Seq data sets of sizes

5 million, 10 million and 20 million reads, covering 1,000 genes randomly selected from the human GENCODE annotation (v19) (Harrow *et al.*, 2012) at various depths. For this analysis, we put our main focus on the sensitive detection of novel alternative splicing events. Thus, we pre-filtered the annotation to genes that had at least two transcripts annotated.

All reads were aligned to the human reference genome using the *STAR* (Dobin *et al.*, 2013) as well as the *TopHat2* (Kim *et al.*, 2013) aligners to show the applicability of our pipeline in a general context. In both cases, we provided the full reference annotation for index creation. *TopHat2* implements a 2-pass alignment mode per default. As this mode is optional for *STAR*, we ran it with and without 2-pass mode to also get a better understanding of its benefits. In addition to the alignment output, we also transformed the simulated read alignments into BAM format and used it as optimal input for the splice prediction tools, best reflecting ground truth information.

To simulate a realistic scenario of detecting novel AS events based on the provided RNA-Seq alignments only, we provided only a reduced annotation to the tools performing the AS event prediction. This reduced representation contains only the first annotated transcript of a gene, where first is defined as first occurrence in the complete annotation file.

For further details on data set creation and alignment, including all command line parameter settings, we refer to Supplemental Section D.

Differential Analysis The simulated data for the analysis of differential testing was taken from the publication of *rDiff* (Drewe *et al.*, 2013), a tool for the detection of differentially expressed transcripts from RNA-Seq data. The two datasets consist of 5,785 genes each, where half of the genes shows differential relative transcript expression and the other half does not. The *rDiff* publication gives further details on dataset generation.

4.2 Evaluation

Detection of Novel Events We used the *Astalavista* toolbox (Foissac and Sammeth, 2007) to extract all annotated alternative splicing events from the set of the randomly chosen 1,000 genes that we used for data simulation. In contrast to the individual prediction tasks, *Astalavista* had access to all annotated transcripts of a gene and thus generated our ground truth set used for evaluation later on. *Astalavista* generates output following a well-defined nomenclature (Guigó Serra *et al.*, 2008).

The single AS event predictors were run on the limited annotation containing only the first transcript but had access to the RNA-Seq data generated from the non-constrained annotation set. We then converted the output of all other tools into the well defined *Astalavista* format to allow for an easy comparison. For each of the four AS event types (exon skip, intron retention, alternative 3' splice site and alternative 5' splice site), we compared the predictions to the ground truth set and computed precision, recall and F-score metrics.

For this evaluation we considered *JuncBase*, *rMATS*, *SpliceGrapher* and *SplAdder*.

Event Quantification Based on the read data simulated for the detection of novel events, we were also able to evaluate the event quantifications provided by the respective approaches. We based all our analyses an percent spliced in (PSI) values, as they are an accepted standard in the community. To generate the ground truth PSI values, we took the relative expression of a transcript for each gene as simulated by *FluxSimulator*. For each alternative splicing event, we computed its PSI value as the ratio between the sum of abundances of transcripts that represented the inclusion (e.g., not skipping the exon in an exon skip event) over the sum of abundances of all transcripts containing any of the event exons.

The so generated PSI values were then used as ground truth for comparison of the predicted event quantifications. Only the correctly detected events of each approach could be compared to the ground truth quantifications. We used the Pearson correlation coefficient as a measure of agreement between predicted and true PSI values.

This evaluation was performed for *JuncBase*, *rMATs* and *SplAdder*, as *SpliceGrapher* does not provide quantification values.

Differential Analysis The two test sets taken from (Drewe *et al.*, 2013) contain 5,785 genes each that either do (2,937) or do not (2,938) show differential transcript usage. One dataset shows small variability and the other large variability, which we will further refer to as the *small* and *large* dataset, respectively. For each dataset, we used the set of differential genes as ground truth and counted a prediction as a true positive if the tool found at least one significant AS event in that gene. From this we generated receiver operating characteristic (ROC) curves with increasing significance cut-offs to evaluate each tool's performance.

For this analysis we compared only *rMATS*, *JuncBase* and *SplAdder*, as *SpliceGrapher* does provide no differential testing functionality.

5 RESULTS

5.1 Detection of Novel Events

Based on the three sets of simulated reads and the different alignments performed on these read sets, we evaluated how well the single prediction tools can reconstruct the splicing variability in the sample from read alignments and limited annotation. In comparison to the ground truth dataset generated by using *Astalavista* on the non-restricted annotation file, we computed precision, recall and F-Score metrics for four types of AS events (Figures 2, S-6 and S-7).

In general we find varying accuracies across the different event types, with consistent patterns for all the tested tools. Intron retentions are the most difficult to predict and exon skips the easiest. *rMATS* was able to detect only two kinds of events on the data we provided: exon skips and mutual exclusive exons. Only exon skips were part of our evaluation. All event types that were not predicted are shown as bars of height zero. We also would like to note, that the simulated data resembles a polyA selected library. When working with non-polyA selected, rRNA depleted libraries, performance will likely be worse, as incompletely spliced transcripts will be amongst the sequenced fragments, diluting the signal.

Across all event types, sample sizes and alignment methods *SplAdder* shows the best performance compared to the other tools. Although *rMATS* shows the highest precision on the predicted exon skip events (0.965, cf. Supplemental Fig. S-6), it has a considerably lower recall, thus affecting its overall performance. Further, it does not predict any of the other assessed types. In contrast *JuncBase*

shows a generally high recall but predicts many false positive events, resulting in a low precision (cf. Supplemental Figs. S-6 and S-7).

A high read coverage has, in general, a positive effect on prediction accuracy with better results for the samples covered at a higher depth. However, we observed some instances where high coverage results in lower performance, most likely due to more false positives in the predicted set.

5.2 Event Quantification

For all events that were correctly predicted by each approach, we compared the associated PSI value to the ground truth computed on the simulated abundances.

In general, we observe good correlation between predicted and true PSI values (cf. Supplemental Table F for a list of all coefficients). Whereas *SplAdder* shows the highest correlation for exon skip events, *JuncBase* has slightly higher accuracy for the other event types, although closely followed by the *SplAdder* predictions. As *rMATS* only predicted exon skip events, we could only include this one event type into our comparison.

We did not observe large differences between correlation values for the different aligners. Interestingly, a higher read depth led to slightly lower quantification accuracies for all tools, even when using the unaligned ground truth read data. We speculate that this is an effect of the simulation tool. However, since we use the reads only for a relative comparison of the different approaches, our evaluation should not suffer from this.

5.3 Differential Analysis

SplAdder can be utilized in two different ways to compare alternative splicing between samples. One approach is to use the event mini-genes output by *SplAdder* as input to other tools for the analysis of differential transcript usage. For our experiments, we use *rDiff* and refer to this use case as *SplAdder+rDiff*. In addition, we recently added a testing module to the *SplAdder* core pipeline that uses a Generalized Linear Model (GLM), which we will refer to as *SplAdder+GLM* in the following evaluations. Based on the two artificial data sets described above, we find that *SplAdder* shows very good performance overall when compared to other testing approaches (Figure 3).

In the range of a low false positive rate, the performance of *SplAdder+rDiff* is comparable to *rMATS* and slightly inferior to *SplAdder+GLM*. This is consistent for both the small and large variance dataset. *JuncBase* uses a t-test for assessing the different groups of samples, which appears less well suited for testing read count data, as it leads to relatively many false positives at high confidence. The ROC curve shape directly reflects this.

5.4 Software and Usability

We have taken great care when implementing the *SplAdder* approach. It has been developed in Matlab but was translated into Python to improve accessibility. Both implementations provide the same functionality, however we will continue future development in Python only. When it comes to usability, *SplAdder* is a convenient one-stop-shop that provides all analysis within a single pipeline. With one simple command line call specifying the parameter set, all subsequent steps are automatized. In addition, the pipeline can be broken into single steps if necessary.

All other tested approaches required invocation of multiple separate tool components and required custom scripting on the user side to form a coherent pipeline. A single exception is *rMATS* that is also well engineered and is quite usable. Most of this also reflects in the running times of the implementations (cf. Supplemental Table E). Whereas *rMATS* and *SplAdder* have quite low running times, *JuncBase* and *SpliceGrapher* are considerably slower. Especially the *Cufflinks* preprocessing for *JuncBase* is very compute intense, with up to 30 hours for some evaluation samples of the largest size. Thus, we have excluded this preprocessing time from the running time table for *JuncBase*.

We believe that *SplAdder*'s improved usability is an important feature that will enable comprehensive AS analysis on RNA-Seq data for a wider audience than with previous methods. Our method is particularly timely, given the ubiquitous precence of available RNA-seq data, high interest in quantifying splicing phenotypes, and scalability to process thousands of samples.

6 CONCLUSION

We present *SplAdder*, a novel approach for the large-scale analysis of alternative splicing events based on RNA-Seq data. We also provide a thoroughly engineered software implementation that is straightforward to use and can be easily deployed in a high performance computing framework. *SplAdder* has been successfully applied to splicing analysis in various organisms, compares favorably to various other state of the art methods showing an overall high accuracy and can be readily applied to datasets of thousands of samples. We are working to further improve *SplAdder* to natively work with high performance compute clusters and generate more interactive visualizations.

Acknowledgements

The authors are grateful to Vipin T Sreedharan for providing code to convert annotation files, to Andreas Wachter for valuable discussions and feedback on the software and to David Kuo for proofreading. *Funding* was provided by the Max Planck Society, Memorial Sloan Kettering Cancer Center, by the German Research Foundation (RA1894/2-1) and the Lucille Castori Center for Microbes, Inflammation, and Cancer (No. 223316).

REFERENCES

Behr, J., Kahles, A., Zhong, Y., Sreedharan, V. T., Drewe, P., and Rätsch, G. (2013). MITIE: Simultaneous RNA-Seq-based transcript identification and quantification in multiple samples. *Bioinformatics*, **29**(20), 2529–2538.

Brooks, A. N., Yang, L., Duff, M. O., Hansen, K. D., Park, J. W., Dudoit, S., Brenner, S. E., and Graveley, B. R. (2011). Conservation of an RNA regulatory map between Drosophila and mammals. *Genome Research*, **21**(2), 193–202.

Dobin, A., Davis, C. a., Schlesinger, F., Drenkow, J., Zaleski, C., Jha, S., Batut, P., Chaisson, M., and Gingeras, T. R. (2013). STAR: ultrafast universal RNA-seq aligner. *Bioinformatics*, **29**(1), 15–21.

Drechsel, G., Kahles, A., Kesarwani, A. K., Stauffer, E., Behr, J., Drewe, P., Rätsch, G., and Wachter, A. (2013). Nonsense-Mediated Decay of Alternative Precursor mRNA Splicing Variants Is a Major Determinant of the Arabidopsis Steady State Transcriptome. *The Plant Cell*, **25**(10), 3726–3742.

Drewe, P., Stegle, O., Hartmann, L., Kahles, A., Bohnert, R., Wachter, A., Borgwardt, K., and Rätsch, G. (2013). Accurate detection of differential RNA processing. *Nucleic Acids Research*, **41**(10), 5189–5198.

Eichner, J., Zeller, G., Laubinger, S., and Rätsch, G. (2011). Support vector machines-based identification of alternative splicing in Arabidopsis thaliana from whole-genome tiling arrays. *BMC Bioinformatics*, **12**(1), 55.

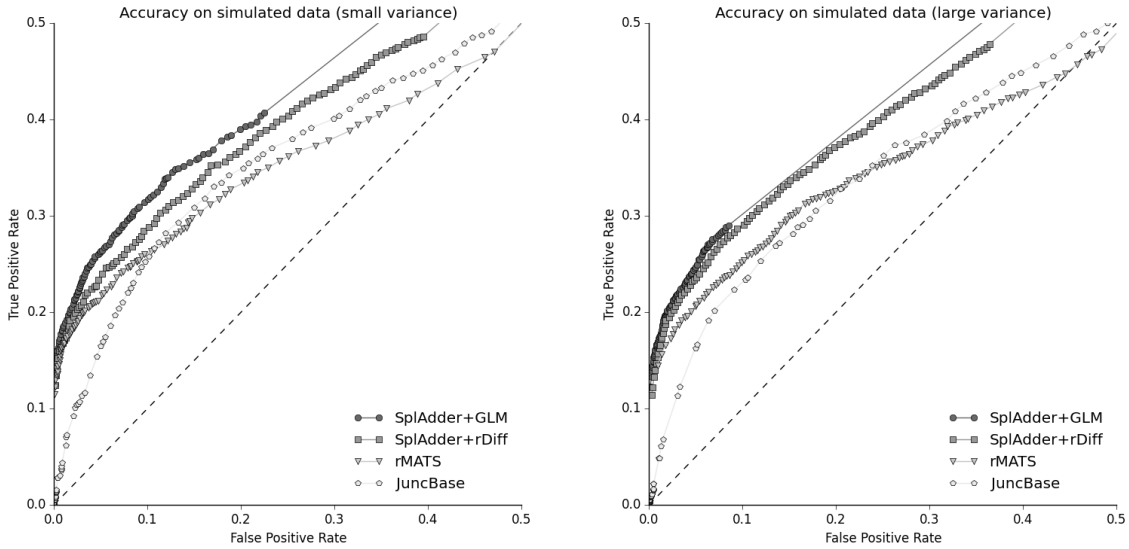

Fig. 3: **Differential Testing Evaluation** Testing accuracy for four different methods (*SplAdder+GLM*, *SplAdder+rDiff*, *rMATS* and *JuncBase*; see legend). Each plot represents a different test set. The plot shown on the left represents the sample dataset with small biological variance between replicates, whereas the plot on the right is based on the sample set with increased biological variance between replicates. The dashed line represents the diagonal and reflects the performance of a random assignment of classes.

Foissac, S. and Sammeth, M. (2007). Astalavista: dynamic and flexible analysis of alternative splicing events in custom gene datasets. *Nucleic acids research*, **35**(suppl 2), W297–W299.

Gan, X., Stegle, O., Behr, J., Steffen, J. G., Drewe, P., Hildebrand, K. L., Lyngsoe, R., Schultheiss, S. J., Osborne, E. J., Sreedharan, V. T., Kahles, A., Bohnert, R., Jean, G., Derwent, P., Kersey, P., Belfield, E. J., Harberd, N. P., Kemen, E., Toomajian, C., Kover, P. X., Clark, R. M., Rätsch, G., and Mott, R. (2011). Multiple reference genomes and transcriptomes for Arabidopsis thaliana. *Nature*, **108**(25), 10249–10254.

Griebel, T., Zacher, B., Ribeca, P., Raineri, E., Lacroix, V., Guigó, R., and Sammeth, M. (2012). Modelling and simulating generic RNA-Seq experiments with the flux simulator. *Nucleic Acids Research*, **40**(20), 10073–10083.

Guigó Serra, R., Sammeth, M., and Foissac, S. (2008). A general definition and nomenclature for alternative splicing events. *PLoS Computational Biology 2008; 4 (8): e1000147*.

Guttman, M., Garber, M., Levin, J. Z., Donaghey, J., Robinson, J., Adiconis, X., Fan, L., Koziol, M. J., Gnirke, A., Nusbaum, C., Rinn, J. L., Lander, E. S., and Regev, A. (2010). Ab initio reconstruction of cell type-specific transcriptomes in mouse reveals the conserved multi-exonic structure of lincRNAs. *Nature Biotechnology*, **28**(5), 503–510.

Harrow, J., Frankish, A., Gonzalez, J. M., Tapanari, E., Diekhans, M., Kokocinski, F., Aken, B. L., Barrell, D., Zadissa, A., Searle, S., Barnes, I., Bignell, A., Boychenko, V., Hunt, T., Kay, M., Mukherjee, G., Rajan, J., Despacio-Reyes, G., Saunders, G., Steward, C., Harte, R., Lin, M., Howald, C., Tanzer, A., Derrien, T., Chrast, J., Walters, N., Balasubramanian, S., Pei, B., Tress, M., Rodriguez, J. M., Ezkurdia, I., van Baren, J., Brent, M., Haussler, D., Kellis, M., Valencia, A., Reymond, A., Gerstein, M., Guigo, R., and Hubbard, T. J. (2012). GENCODE: The reference human genome annotation for The ENCODE Project. *Genome Research*, **22**(9), 1760–1774.

Heber, S., Alekseyev, M., and Sze, S. (2002). Splicing graphs and est assembly problem. *Bioinformatics*, **18**, 181–188.

Katz, Y., Wang, E. T., Airoldi, E. M., and Burge, C. B. (2010). Analysis and design of RNA sequencing experiments for identifying isoform regulation. *Nature Methods*, **7**(12), 1009–1015.

Kianianmomeni, A., Ong, C. S., Rätsch, G., and Hallmann, A. (2014). Genome-wide analysis of alternative splicing in volvox carteri. *BMC genomics*, **15**(1), 1117.

Kim, D., Pertea, G., Trapnell, C., Pimentel, H., Kelley, R., and Salzberg, S. L. (2013). TopHat2: accurate alignment of transcriptomes in the presence of insertions, deletions and gene fusions. *Genome Biology*, **14**(4), R36.

Kornblihtt, A. R., Schor, I. E., Alló, M., Dujardin, G., Petrillo, E., and Muñoz, M. J. (2013). Alternative splicing: a pivotal step between eukaryotic transcription and translation. *Nature Reviews Molecular Cell Biology*, **14**(3), 153–165.

Love, M. I., Huber, W., and Anders, S. (2014). Moderated estimation of fold change and dispersion for rna-seq data with deseq2. *Genome Biol*, **15**(12), 550.

Modrek, B. and Lee, C. (2002). A genomic view of alternative splicing. *Nature Genetics*, **30**(1), 13–19.

Pan, Q., Shai, O., Lee, L. J., Frey, B. J., and Blencowe, B. J. (2008). Deep surveying of alternative splicing complexity in the human transcriptome by high-throughput sequencing. *Nature Genetics*, **40**(12), 1413–1415.

Reyes, A., Anders, S., and Huber, W. (2012). Detecting differential usage of exons from RNA-Seq data. *Genome Research*, **22**, 2008–2017.

Rogers, M. F., Thomas, J., Reddy, A. S., and Ben-Hur, A. (2012). SpliceGrapher: detecting patterns of alternative splicing from RNA-Seq data in the context of gene models and EST data. *Genome Biology*, **13**(1), R4.

Shen, S., Park, J. W., Lu, Z.-x., Lin, L., Henry, M. D., Wu, Y. N., Zhou, Q., and Xing, Y. (2014). rmats: Robust and flexible detection of differential alternative splicing from replicate rna-seq data. *Proceedings of the National Academy of Sciences*, **111**(51), E5593–E5601.

Trapnell, C., Williams, B. A., Pertea, G., Mortazavi, A., Kwan, G., van Baren, M. J., Salzberg, S. L., Wold, B. J., and Pachter, L. (2010). Transcript assembly and quantification by RNA-Seq reveals unannotated transcripts and isoform switching during cell differentiation. *Nature Biotechnology*, **28**(5), 511–515.

Wang, E. T., Sandberg, R., Luo, S., Khrebtukova, I., Zhang, L., Mayr, C., Kingsmore, S. F., Schroth, G. P., and Burge, C. B. (2008). Alternative isoform regulation in human tissue transcriptomes. *Nature*, **456**(7221), 470–476.

Weinstein, J. N., Collisson, E. a., Mills, G. B., Shaw, K. R. M., Ozenberger, B. a., Ellrott, K., Shmulevich, I., Sander, C., and Stuart, J. M. (2013). The Cancer Genome Atlas Pan-Cancer analysis project. *Nature Genetics*, **45**(10), 1113–1120.

Wu, J., Akerman, M., Sun, S., McCombie, W. R., Krainer, A. R., and Zhang, M. Q. (2011). Splicetrap: a method to quantify alternative splicing under single cellular conditions. *Bioinformatics*, **27**(21), 3010–3016.

Supplementary Material

SplAdder: Identification, quantification and testing of alternative splicing events from RNA-Seq data

André Kahles,[1] Cheng Soon Ong,[2] Yi Zhong,[1] and Gunnar Rätsch[1]

[1]Computational Biology Center, Sloan Kettering Institute, 1275 York Ave, New York, NY 10067, USA
[2]NICTA, Canberra Research Laboratory, Tower A, 7 London Circuit, Canberra ACT 2601, Australia

The following paragraphs provide additional details to certain parts that are only briefly summarized in the main text. The first section provides further details on step four of the graph augmentation process, describing which rules are applied to add novel intron edges. The second section formally defines the splicing events that can be extracted from a given splicing graph and gives a verbal summary of the algorithms detecting each event type. The subsequent sections describe the model used for differential analysis between groups of samples and the procedures that we followed for test data generation and evaluation. The final section gives a brief overview on available visualizations of splicing patterns and event quantifications.

A SPLICING GRAPH AUGMENTATION

The augmentation of the splicing graph comprises several iterative steps, that are described in the main text. Here, we provide additional details on step four of the algorithm, the addition of novel intron edges into the graph.

In the following, we formally define all cases to insert new intron edges into the graph.

1. To handle the first case we split it into three sub-cases:

   a. If the intron (g_i, g_j) is fully contained within an existing node ($\exists v \in \hat{V} : g_i > g_{v,\text{start}}$ and $g_j < g_{v,\text{end}}$), we can insert a new intron into the node, thus creating two new nodes $v_{n_1} = (g_{v,\text{start}}, g_i - 1)$ and $v_{n_2} = (g_j + 1, g_{v,\text{end}})$. After adding v_{n_1} and v_{n_2} to $\hat{V}$, we update the edge set to

$$\begin{aligned}\hat{E} = \hat{E} &\cup \{(v_{n_1}, v_{n_2})\} \\ &\cup \bigcup_{x \in \hat{V}} \left\{(x, v_{n_1}) \mid (x, v) \in \hat{E}\right\} \\ &\cup \bigcup_{x \in \hat{V}} \left\{(v_{n_2}, x) \mid (v, x) \in \hat{E}\right\}\end{aligned}$$

   b. If the intron (g_i, g_j) is fully contained within an existing intron, we connect it to the two nodes v_s and v_t flanking the containing intron, thus introducing two new nodes $v_{n_1} = (g_{v_s,\text{start}}, g_i - 1)$ and $v_{n_2} = (g_j + 1, g_{v_t,\text{end}})$ into $\hat{V}$. Again, the new nodes inherit their edges from v_s and v_t. This results in the following update rule for the edge set:

$$\begin{aligned}\hat{E} = \hat{E} &\cup \{(v_{n_1}, v_{n_2})\} \\ &\cup \bigcup_{x \in \hat{V}} \left\{(x, v_{n_1}) \mid (x, v_s) \in \hat{E}\right\} \\ &\cup \bigcup_{x \in \hat{V}} \left\{(v_{n_2}, x) \mid (v_t, x) \in \hat{E}\right\}\end{aligned}$$

   c. If one of the intron boundaries (g_i, g_j) is in close proximity (we use $\leq$ 40 nt as a default threshold) to a terminal node, this node is extended to a new node v_{n_1} and a new terminal node v_{n_2} is added to the graph at the other side of the intron. The length k of the new terminal exon is predefined to be 200 nt. If the nearby node v is start-terminal, $v_{n_1} = (g_j + 1, g_{v,\text{end}})$ and $v_{n_2} = (g_i - k - 1, g_i - 1)$ and

$$\hat{E} = \hat{E} \cup \{(v_{n_2}, v_{n_1})\} \cup \bigcup_{x \in \hat{V}} \left\{(v_{n_1}, x) \mid (v, x) \in \hat{E}\right\}.$$

   If the nearby node v is end-terminal, $v_{n_1} = (g_{v,\text{start}}, g_i - 1)$ and $v_{n_2} = (g_j + 1, g_j + k + 1)$ and

$$\hat{E} = \hat{E} \cup \{(v_{n_1}, v_{n_2})\} \cup \bigcup_{x \in \hat{V}} \left\{(x, v_{n_1}) \mid (x, v) \in \hat{E}\right\}.$$

2. The second case is similar in its handling to case 1c). If the start of intron (g_i, g_j) coincides with the end of an existing node v, we distinguish two sub-cases.

   a. There exists a node v' in close proximity to intron-end g_j and we can add a new node $v_n = (g_j + 1, g_{v',\text{end}})$ and update the edge set to

$$\hat{E} = \hat{E} \cup \{(v, v_n)\} \cup \bigcup_{x \in \hat{V}} \left\{(v_n, x) \mid (v', x) \in \hat{E}\right\}.$$

   b. There is no node in close proximity to intron-end g_j, thus we introduce a new end-terminal node $v_n = (g_j + 1, g_j + k + 1)$ and update the edge set to $\hat{E} = \hat{E} \cup \{(v, v_n)\}$.

3. The third case is analogous to case 2). If the end of intron (g_i, g_j) coincides with the start of an existing node v in the graph, we again distinguish two sub-cases.

   a. There exists a node v' in close proximity to g_i and we can add a new node $v_n = (g_{v',\text{start}}, g_i - 1)$ and update the edge set to

$$\hat{E} = \hat{E} \cup \{(v_n, v)\} \cup \bigcup_{x \in \hat{V}} \left\{(x, v_n) \mid (x, v') \in \hat{E}\right\}.$$

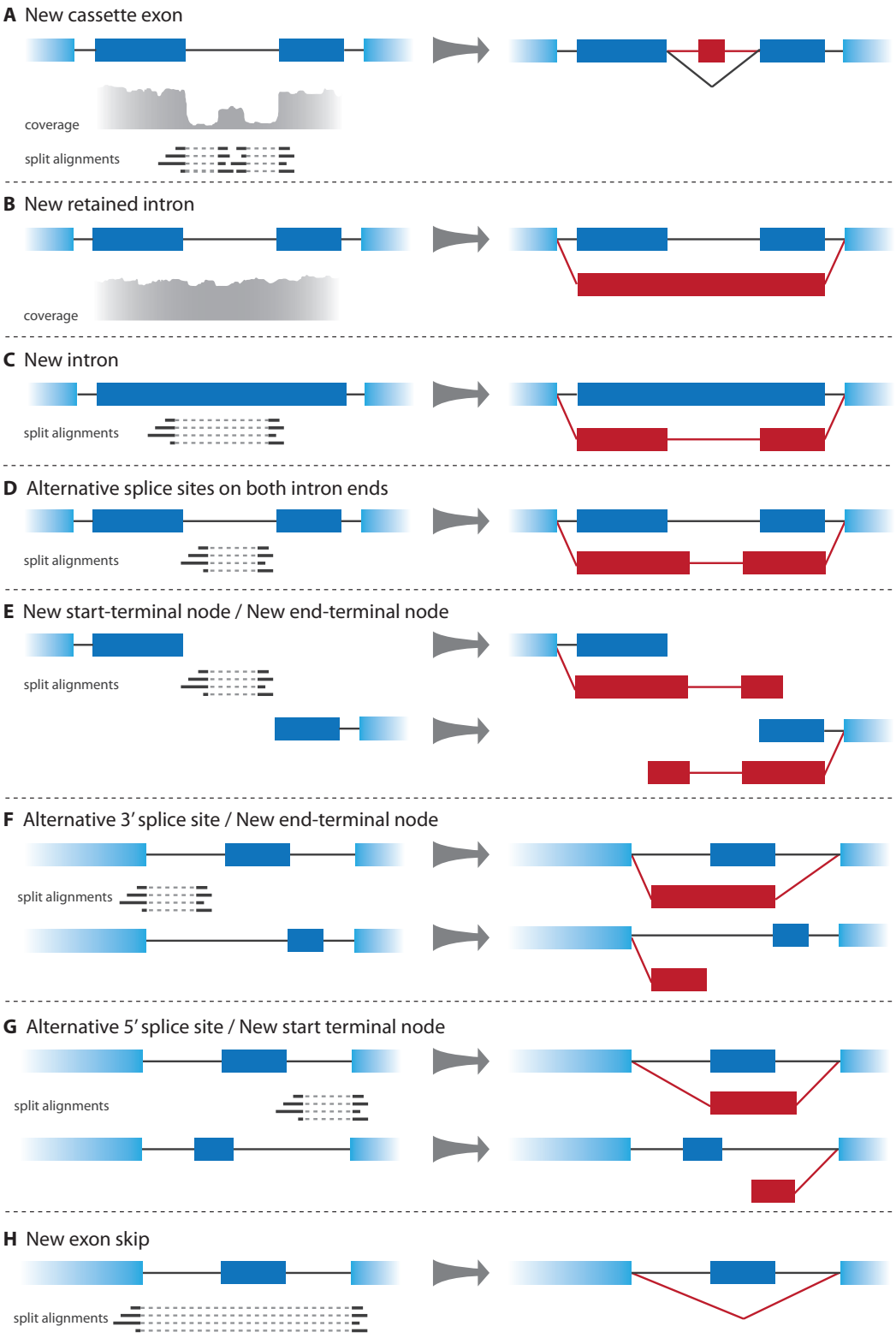

Fig. S-1: Overview of the different classes of splicing graph augmentation. Panels ***A–H*** show all possibilities of how the splicing graph can be augmented within *SplAdder*, based on evidence from RNA-Seq alignment data. In cases where no coverage evidence is shown, only junction confirmations by split alignments are used.

b. There is no node in close proximity to intron-start g_i, thus we introduce a new start-terminal node $v_n = (g_i - k - 1, g_i - 1)$ and update the edge set to $\hat{E} = \hat{E} \cup \{(v_n, v)\}$.

4. The last case is the most straightforward to handle. If intron (g_i, g_j) coincides with the end of node v and the start of node v', we augment the edge set $\hat{E} = \hat{E} \cup \{(v, v')\}$, if the edge is not already present in $\hat{E}$.

B EVENT EXTRACTION AND FILTERING

Here we provide further details on how the respective event types are defined in the context of a splicing graph, how they can be extracted and what filters exist to generate a high confidence set of events.

B.1 Extraction of Alternative Spicing Events

This section formally defines all alternative splicing events as sub-graphs of the splicing graph. For each event type we also briefly describe the algorithm to identify such sub-graphs.

Starting with the augmented splicing graph $\hat{G} = (\hat{V}, \hat{E})$, we can extract the AS event sub-graphs as follows:

Exon Skips are all sub-graphs

$$(V', E') = (\{v_i, v_j, v_k\}, \{(v_i, v_j), (v_j, v_k), (v_i, v_k)\})$$

with $V' \subseteq \hat{V}$ and $E' \subseteq \hat{E}$.

For extraction, we iterate over the list of all sorted nodes and check for each subset of size three, whether all three edges are preset in the edge set. When all conditions are met, the exon set is added to the exon skip event list.

Intron Retentions are all sub-graphs

$$(V', E') = (\{v_i, v_j, v_k\}, \{(v_i, v_j)\})$$

with $V' \subseteq \hat{V}$ and $E' \subseteq \hat{E}$ and $g_{v_i,\text{start}} = g_{v_k,\text{start}}$ and $g_{v_j,\text{end}} = g_{v_k,\text{end}}$.

To extract intron retention events, we iterate over all edges of the graph and check whether any node fully overlaps that edge. Only the first overlapping node is stored.

Alternative 3' Splice Sites are all sub-graphs

$$(V', E') = (\{v_i, v_j, v_k\}, \{(v_i, v_j), (v_i, v_k)\})$$

with $V' \subseteq \hat{V}$ and $E' \subseteq \hat{E}$ and $g_{v_j,\text{end}} = g_{v_k,\text{end}}$. This definition assumes the direction of transcription to be positive. For transcripts from the negative strand, the definitions for alternative 3' splice site and alternative 5' splice site (below) need to be switched.

To identify alternative 3' splice site usage, we iterate through all nodes of the graph of a gene on the plus (minus) strand and check whether it is connected to two overlapping nodes that are downstream (upstream) to it. Both nodes have to overlap by a minimum number of positions. The current default is 11. When a node is connected to more than two nodes, we will iterate over all pairs of overlapping nodes and extract them as individual events.

Alternative 5' Splice Sites are all sub-graphs

$$(V', E') = (\{v_i, v_j, v_k\}, \{(v_i, v_k), (v_j, v_k)\})$$

with $V' \subseteq \hat{V}$ and $E' \subseteq \hat{E}$ and $g_{v_i,\text{start}} = g_{v_j,\text{start}}$. The different strands are handled analogously to alternative 3'-splice sites.

Also the procedure to identify alternative 5' splice site usage is analog to the alternative 3' case. The only difference is that for genes on the plus (minus) strand the upstream (downstream) nodes are considered as alternatives.

Multiple Exon Skips are all sub-graphs

$$(V', E') = (\{v_i, v_{j_1}, \ldots, v_{j_s}, v_k\}, \{(v_i, v_{j_1}), (v_{j_s}, v_k), (v_i, v_k)\} \cup \bigcup_{l=1}^{s-1} \{(v_{j_l}, v_{j_{l+1}})\})$$

with $V' \subseteq \hat{V}$ and $E' \subseteq \hat{E}$.

To identify multiple exon skips, we use the upper triangular matrix of the adjacency matrix of the splicing graph. (The adjacency matrix for the splicing graph is a square binary matrix A with one row/column per node. An entry $A_{i,j}$ is 1 when there is an edge between nodes v_i and v_j and 0 otherwise). Through iteratively multiplying this matrix to itself, we iterate through all paths of increasing length. When we find a path where first and last node are connected by an edge, we have found a multiple exon skip. For all such pairs, we use the shortest path as inclusion splice form.

Mutually Exclusive Exons are all sub-graphs

$$(V', E') = (\{v_i, v_j, v_k, v_l\}, \{(v_i, v_j), (v_i, v_k), (v_j, v_l), (v_k, v_l)\})$$

with $V' \subseteq \hat{V}$ and $E' \subseteq \hat{E}$ and $(v_j, v_k) \notin \hat{E}$ and $v_j \neq v_k$.

For the identification of mutually exclusive exons, we iterate through all nodes and check for each node, whether it has edges to two downstream nodes that again themselves have edges to a common downstream node. All such sets of 4 nodes will be extracted as mutually exclusive exon events.

The same extraction rules would apply to extract alternative splicing events from the not augmented graph G. A schematic overview of the extraction process is provided in Figure S-3.

B.2 Event Filtering and Quantification

Alternative splicing events extracted from the graph are filtered at several levels. To remove redundant events, all events are made unique based on their inner event coordinates. The inner event coordinates are defined as the start and end positions of all introns of the event. If two events share the same inner coordinates, they are replaced by a new event with the same inner coordinates but adapted outer coordinates, minimizing the total length of the event. An example for this is shown in Figure S-4. Events in Panel A can be merged, whereas events in Panel B disagree in their inner coordinates and remain separate.

Next, we use the RNA-Seq data to quantify each of the extracted events. That is, for each intron we count the number of alignments supporting it and compute the mean coverage c for each exon. For reasons of computational efficiency, the quantification is performed on the segment graph. As defined in the main text, each segment can be uniquely identified by its genomic coordinates. Thus, we extract

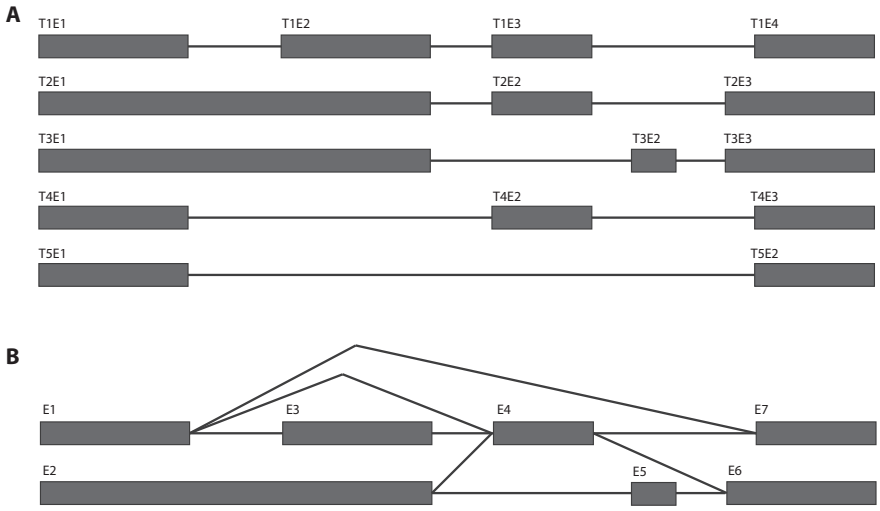

Fig. S-2: Example case for the construction of a splicing graph. ***A:*** Set of five different transcripts of a gene. Exons are depicted as gray boxes and introns as solid lines. Labels TiEj denote exon j in transcript i. ***B:*** Splicing graph representation of the same five transcripts. Exons occurring in multiple transcripts are collapsed into a single exon in the graph (e.g., exons T1E3, T2E2, and T4E2 are collapsed into node E4).

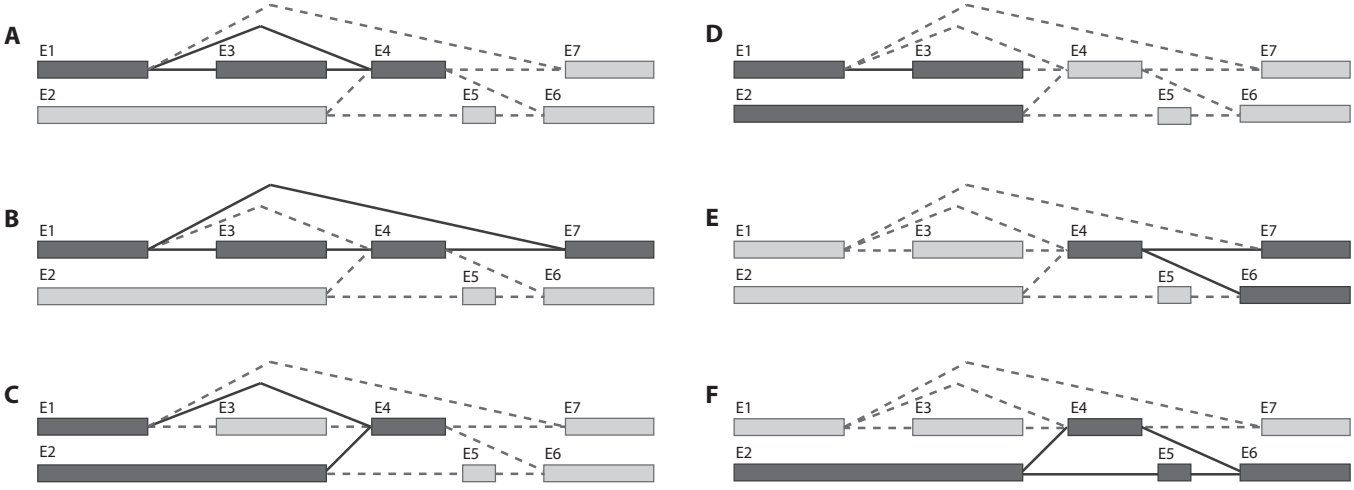

Fig. S-3: Six different types of alternative splicing events are currently extracted from the splicing graph. The graph structure is given with nodes as gray boxes and edges as solid/dashed lines. Solid/dark parts show the event of interest and light/dashed parts the remainder of the graph structure. ***A:*** Exon skip, ***B:*** Multiple exon skip, ***C:*** Alternative 5' splice site, ***D:*** Intron retention, ***E:*** Alternative 3' splice site, ***F:*** Mutually exclusive exons.

for each node its mean coverage and for each edge the number of spliced alignments in the sample confirming this edge. As each exon v_i can be formed through a concatenation of segments $s_q \circ s_r$, we can use the segment-lengths and their average coverage to compute the average coverage of the exon:

$$c_{v_i} = \frac{\sum_{j=q}^{r}(g_{s_j,\text{end}} - g_{s_j,\text{start}} + 1) \cdot c_{s_j}}{\sum_{j=q}^{r}(g_{s_j,\text{end}} - g_{s_j,\text{start}} + 1)},$$

where $s_q \circ s_r$ is the sequence of segments contained in node v_i.

In many applications, the splicing graphs can grow very complex, containing alternative events that are only poorly supported by input data. Thus, we use the quantifications to further filter the event set and to only retain the most confident events. Each event type has a different set of criteria it has to fulfill in order to become a valid event. Complete listings of the respective criteria are provided in Table D. To determine whether an event is valid, the algorithm checks in which of the provided RNA-Seq samples which criteria are met. An event is valid, if all criteria are met in at least one sample. To create more stringently filtered sets of events, this threshold can be increased. In general, most of the *SplAdder* thresholds can be adapted, allowing for fine tuning towards a respective task.

C DIFFERENTIAL TESTING OF AS-EVENTS

When multiple groups of samples are present, *SplAdder* can test for significant differences in event expression between samples. Here, we provide further details on our model used for testing.

We use a negative binomial distribution to approximate the expression or splicing read count y for each splicing event i:

$$y^i \sim NB(\mu^i, \kappa^i),$$

where μ^i is the expected count and κ^i is the estimated dispersion across samples. We formulate the problem as a generalized linear model (GLM) to estimate the μ^i given the observed counts y^i. In the GLM, the expected counts are decomposed into several representative latent quantities β^i. Under the null hypothesis, the expected count μ^i is given as

$$\log(\mu^i) = \beta_0^i + \beta_{\text{expr}}^i + \beta_{\Delta\ \text{expr}}^i,$$

where β_0^i is the coefficient denoting the intercept; β_{expr}^i is the contribution of the observed count to the μ^i due to gene expression; $\beta_{\Delta\ \text{expr}}^i$ represents the distinction between two conditions at the expression level. An additional term $\beta_{\Delta\ \text{spl}}^i$ representing the splicing difference (alternative splicing) is included in the alternative hypothesis model as

$$\log(\mu^i) = \beta_0^i + \beta_{\text{expr}}^i + \beta_{\Delta\ \text{expr}}^i + \beta_{\Delta\ \text{spl}}^i.$$

In the GLM model, we test the existence of an alternative splicing effect, taking into account expression as a confounding factor. Firstly, the GLM system is used to obtain the μ^i from the estimated β^i. The κ^i is estimated by maximizing the negative binomial likelihood function given μ^i. Then, to reduce the uncertainty of κ^i estimated from the limited number of replicates, all κ^i are regressed to obtain a function $f(\mu) = \lambda_1/\mu + \lambda_0$ to build a mean-dispersion relationship (Reyes *et al.*, 2012), where λ_1 and λ_0 are the two parameters estimated during the regression. Thirdly, to finalize the κ for each event with μ^i, we adjust the κ towards the $f(\mu)$ using an empirical Bayes shrinkage strategy (Love *et al.*, 2014), thereby reducing the large variance of κ^i. Lastly, the count data are fitted into H_0 and H_1 separately and a χ^2-test is performed based on the difference of deviances of the two GLM fits. We use the Benjamini-Hochberg procedure (Benjamini and Hochberg, 1995) to correct for multiple testing.

D EVALUATION AND TESTING

The *SplAdder* software has been developed in the context of application and has been successfully applied in numerous projects on *Arabidopsis thaliana* (Rühl *et al.*, 2012; Drechsel *et al.*, 2013; Gan *et al.*, 2011) as well as in large scale sequencing projects on human RNA-Seq samples taken from cancer patients (Weinstein *et al.*, 2013). However, to allow for an accurate measure of performance, we have used simulated data in this work to assess the *SplAdder* results.

As described in the main text, we used the *FluxSimulator* (version 1.1.1-20121103021450) (Griebel *et al.*, 2012) to simulate RNA-Seq reads. For all three sample set sizes, we used the software with its recommended settings. As previously described, the reads were sampled from an annotation file containing 1,000 genes randomly selected from a pre-filtered version of the Genocde (v19) annotation, that only contained genes with multiple transcripts annotated. The read simulations produced 100 nt paired-end reads when using the following parameters:

```
EXPRESSION_X0        9500
EXPRESSION_K         -0.6
TSS_MEAN             50
POLYA_SCALE          300
POLYA_SHAPE          2
FRAG_SUBSTRATE       DNA
FRAG_METHOD          NB
FRAG_NB_LAMBDA       500
FILTERING            YES
SIZE_DISTRIBUTION    N-300-50.txt
SIZE_SAMPLING        AC
RTRANSCRIPTION       YES
PCR_PROBABILITY      0.7
RT_PRIMER            PDT
RT_LOSSLESS          YES
RT_MIN               500
RT_MAX               5500
PAIRED_END           YES
FASTA                YES
```

Where `N-300-50.txt` contains a random sample, drawn from a normal distribution with mean 300 and standard deviation 50. We used the above settings for all three sample set sizes, only adapting the total number of reads sampled.

These reads were aligned back to the hg19 reference genome sequence using the *TopHat2* (Kim *et al.*, 2013) and *STAR* (Dobin *et al.*, 2013) aligners. *STAR* was run in default mode as well as a 2-pass alignment mode that detects novel splice junctions in a first run and uses this information in a second alignment run.

TopHat2 was run with the following set of parameters (settings not mentioned were left at their default):

```
--GTF <annotation_file>
--num-threads 8
--read-gap-length 3
--read-edit-dist 5
-o <out_directory>
-r 200
--min-intron-length 40
--max-intron-length 500000
--no-discordant
```

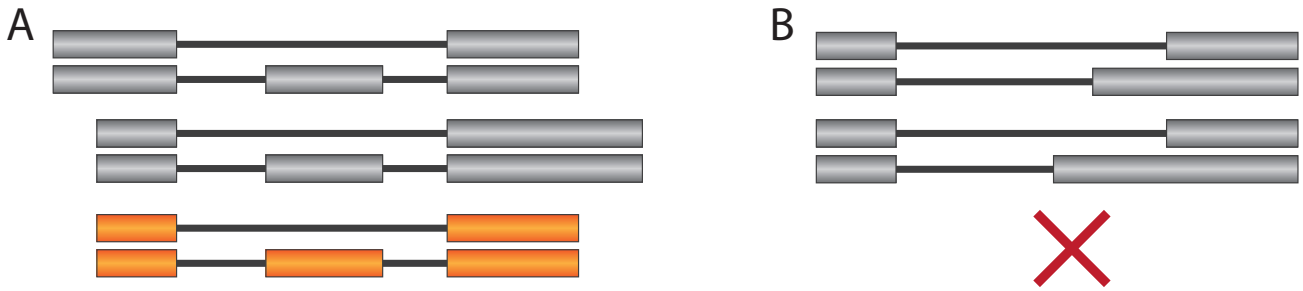

Fig. S-4: Example cases describing whether overlapping events can be merged or not. ***A:*** All inner event coordinates agree and the events can be successfully merged. ***B:*** Both events have only one intron in common, whereas the other introns disagree. The events cannot be merged and remain separate.

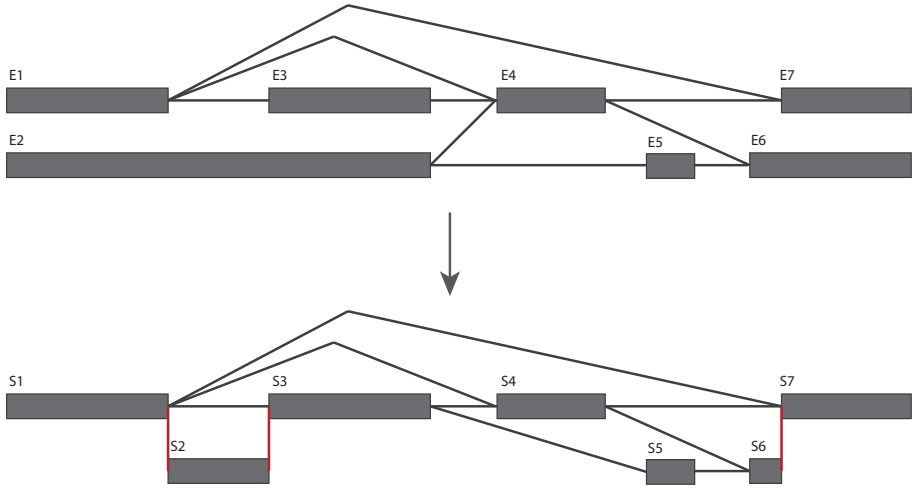

Fig. S-5: Transformation of a splicing graph into a segment graph representation. Gray boxes represent nodes, black lines intron edges and red lines non-intron edges that encode the relationship between segments and splicing graph nodes.

```
--microexon-search
```

STAR in its default mode was run with the following set of parameters (settings not mentioned were left at their default):

```
--runThreadN 4
--genomeDir <genome_dir>
--genomeLoad NoSharedMemory
--readFilesIn <fastq_files>
--readFilesCommand zcat
--limitBAMsortRAM 70000000000
--outSAMtype BAM Unsorted
--outSAMstrandField intronMotif
--outSAMattributes NH HI NM MD AS XS
--outSAMheaderHD @HD   VN:1.4
--outFilterMultimapNmax 50
--outFilterMultimapScoreRange 3
--outFilterScoreMinOverLread 0.7
--outFilterMatchNminOverLread 0.7
--outFilterMismatchNmax 10
--alignIntronMax 500000
--alignMatesGapMax 1000000
--sjdbScore 2
```

For *STAR* in 2-pass mode, we used the parameters as above and added the following setting:

```
--twopassMode Basic
```

For sorting and indexing alignment files in BAM format we used *Samtools* (Li *et al.*, 2009) (version 0.1.20).

As described in the main text, to focus on the prediction of novel splicing events, we removed all but the first transcript from each gene and stored this as a *backbone annotation*, which was then provided to *SplAdder* as well as the other tools along with the simulated read sets.

To assess how much complexity could be restored by the various tools, we generated a ground truth dataset from the unrestricted annotation file that was used for data simulation using the *Astalavista* toolbox (Foissac and Sammeth, 2007).

We converted the output of all tools into the format described in (Guigó Serra *et al.*, 2008) using custom scripts. Based on the overlap of the predicted events and the ground truth events, we were able to identify true positives and false positives and thus compute precision, recall and F-Score metrics. An overview of the F-Score for all tools and data sets is presented in the main text. The same overview for precision and recall is shown in supplemental Figures S-6 and S-7, respectively.

SplAdder was run with the following set of parameters for all analyses shown:

```
spladder.py
    -b <bam_files>
    -o <out_directory>
    -a <annotation_gff>
    -v y
    -c 3
    -M merge_graphs
    -T y
    -V n
    -n 100
    -P y
    -p n
    -t exon_skip,intron_retention,alt_3prime,
       alt_5prime,mutex_exons,mult_exon_skip
    --output_struc y
```

rMATS was run with the following set of parameters:

```
rmats.py
    -b1 <bam_files>
    -b2 <bam_files>
    -gtf <annotation_gff>
    -o <out_directory>
    -t single
    -len 100
```

The multiple steps of the *JuncBase* pipeline were run according to the tutorial that is described in the `MANUAL.pdf` in the source code of version 0.6. Parameters were chosen as suggested there.

The `samfilter.py` part of *SpliceGrapher* was run with the following parameters:

```
sam_filter.py
    <bam_files>
    <classif>
    -f <genome.fasta>
    -m <annotation.gff>
    -v
    -o <sam_filtered>
```

Where `<classif>` is the classifier for Homo Sapiens provided by the developers of *SpliceGrapher*. Then the prediction step was run with

```
predict_graphs.py
    <sam_filtered>
    -m <annotation_gff>
    -v
    -d <out_directory>
```

The running times of all tools shown in Supplementary Table E were measured on compute nodes in a high performance computing environment consisting of several multi-core machines, using 24 Intel® Xeon® CPU E5-2665 2.40GHz processors, each. All tools were run on a dedicated processor in single-thread mode.

E VISUALIZATIONS

Being able to transform the large amount of splicing information available for a gene locus into an easy to comprehend overview is an important step towards a better understanding of altered splicing mechanisms or to identify impaired RNA regulation. To aid with this, *SplAdder* is able to produce a variety of diagnose and overview-plots to summarize information at a specific locus or to given an overview on the distributions of certain characteristics of all identified events.

An illustrative example is the gene-locus overview plot that can summarize the splicing graph of a gene and align it to the coverage in a set of given samples, thereby highlighting coverage differences (cf. Supplemental Figure S-8).

The list of available plotting routines is constantly extended. Please refer to the user documentation and the *SplAdder* wiki for a more comprehensive overview.

REFERENCES

Benjamini, Y. and Hochberg, Y. (1995). Controlling the false discovery rate: a practical and powerful approach to multiple testing. *Journal of the Royal Statistical Society. Series B (Methodological)*, **51**(1), 289 – 300.

Dobin, A., Davis, C. a., Schlesinger, F., Drenkow, J., Zaleski, C., Jha, S., Batut, P., Chaisson, M., and Gingeras, T. R. (2013). STAR: ultrafast universal RNA-seq aligner. *Bioinformatics*, **29**(1), 15–21.

Drechsel, G., Kahles, A., Kesarwani, A. K., Stauffer, E., Behr, J., Drewe, P., Rätsch, G., and Wachter, A. (2013). Nonsense-Mediated Decay of Alternative Precursor mRNA Splicing Variants Is a Major Determinant of the Arabidopsis Steady State Transcriptome. *The Plant Cell*, **25**(10), 3726–3742.

Foissac, S. and Sammeth, M. (2007). Astalavista: dynamic and flexible analysis of alternative splicing events in custom gene datasets. *Nucleic acids research*, **35**(suppl 2), W297–W299.

Gan, X., Stegle, O., Behr, J., Steffen, J. G., Drewe, P., Hildebrand, K. L., Lyngsoe, R., Schultheiss, S. J., Osborne, E. J., Sreedharan, V. T., Kahles, A., Bohnert, R., Jean, G., Derwent, P., Kersey, P., Belfield, E. J., Harberd, N. P., Kemen, E., Toomajian, C., Kover, P. X., Clark, R. M., Rätsch, G., and Mott, R. (2011). Multiple reference genomes and transcriptomes for Arabidopsis thaliana. *Nature*, **108**(25), 10249–10254.

Griebel, T., Zacher, B., Ribeca, P., Raineri, E., Lacroix, V., Guigó, R., and Sammeth, M. (2012). Modelling and simulating generic RNA-Seq experiments with the flux simulator. *Nucleic Acids Research*, **40**(20), 10073–10083.

Guigó Serra, R., Sammeth, M., and Foissac, S. (2008). A general definition and nomenclature for alternative splicing events. *PLoS Computational Biology 2008; 4 (8): e1000147*.

Kim, D., Pertea, G., Trapnell, C., Pimentel, H., Kelley, R., and Salzberg, S. L. (2013). TopHat2: accurate alignment of transcriptomes in the presence of insertions, deletions and gene fusions. *Genome Biology*, **14**(4), R36.

Li, H., Handsaker, B., Wysoker, A., and Fennell, T. (2009). The sequence alignment/map format and SAMtools. *Bioinformatics*, **25**(16), 2078–2079.

Love, M. I., Huber, W., and Anders, S. (2014). Moderated estimation of fold change and dispersion for rna-seq data with deseq2. *Genome Biol*, **15**(12), 550.

Reyes, A., Anders, S., and Huber, W. (2012). Detecting differential usage of exons from RNA-Seq data. *Genome Research*, **22**, 2008–2017.

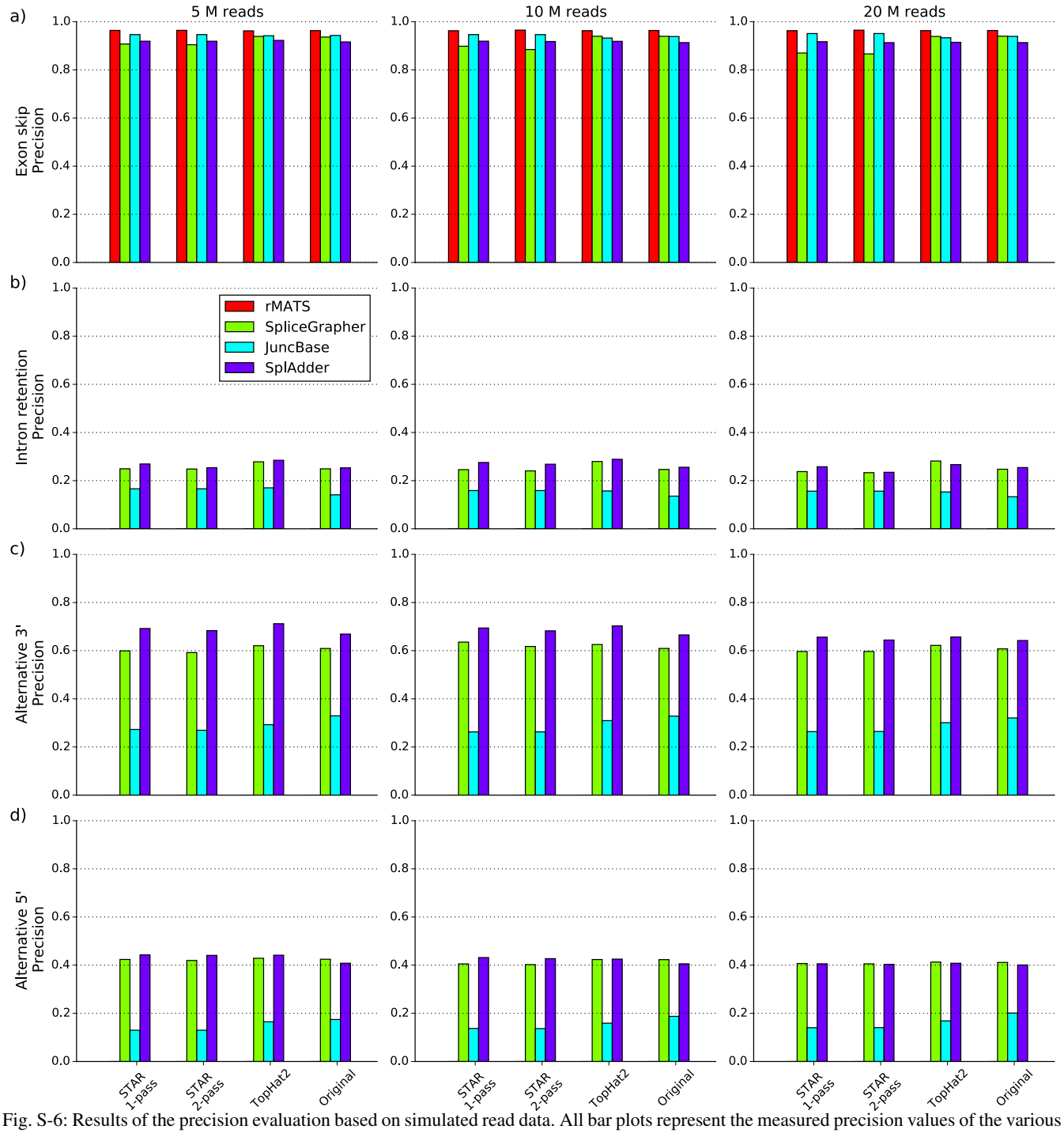

Fig. S-6: Results of the precision evaluation based on simulated read data. All bar plots represent the measured precision values of the various methods compared (*rMATS* (red), *SpliceGrapher* (light green), *JuncBase* (light blue) and *SplAdder* (purple)). Each row represent a different AS event type (from top to bottom: intron retention, exon skip, alternative 3' splice site and alternative 5' splice site) and each column represents a different sample size (from left to right: 5×10^6, 10×10^6, 20×10^6). The groups of bars in the single charts show the different aligners used: (from left to right: *STAR 1-pass*, *STAR 2-pass*, *TopHat*, and the ground truth alignments).

Rühl, C., Stauffer, E., Kahles, A., Wagner, G., Drechsel, G., Rätsch, G., and Wachter., A. (2012). Polypyrimidine Tract Binding Protein Homologs from Arabidopsis Are Key Regulators of Alternative Splicing with Implications in Fundamental Developmental Processes. *The Plant Cell*, **24**(11), 4360–4375.

Weinstein, J. N., Collisson, E. a., Mills, G. B., Shaw, K. R. M., Ozenberger, B. a., Ellrott, K., Shmulevich, I., Sander, C., and Stuart, J. M. (2013). The Cancer Genome Atlas Pan-Cancer analysis project. *Nature Genetics*, **45**(10), 1113–1120.

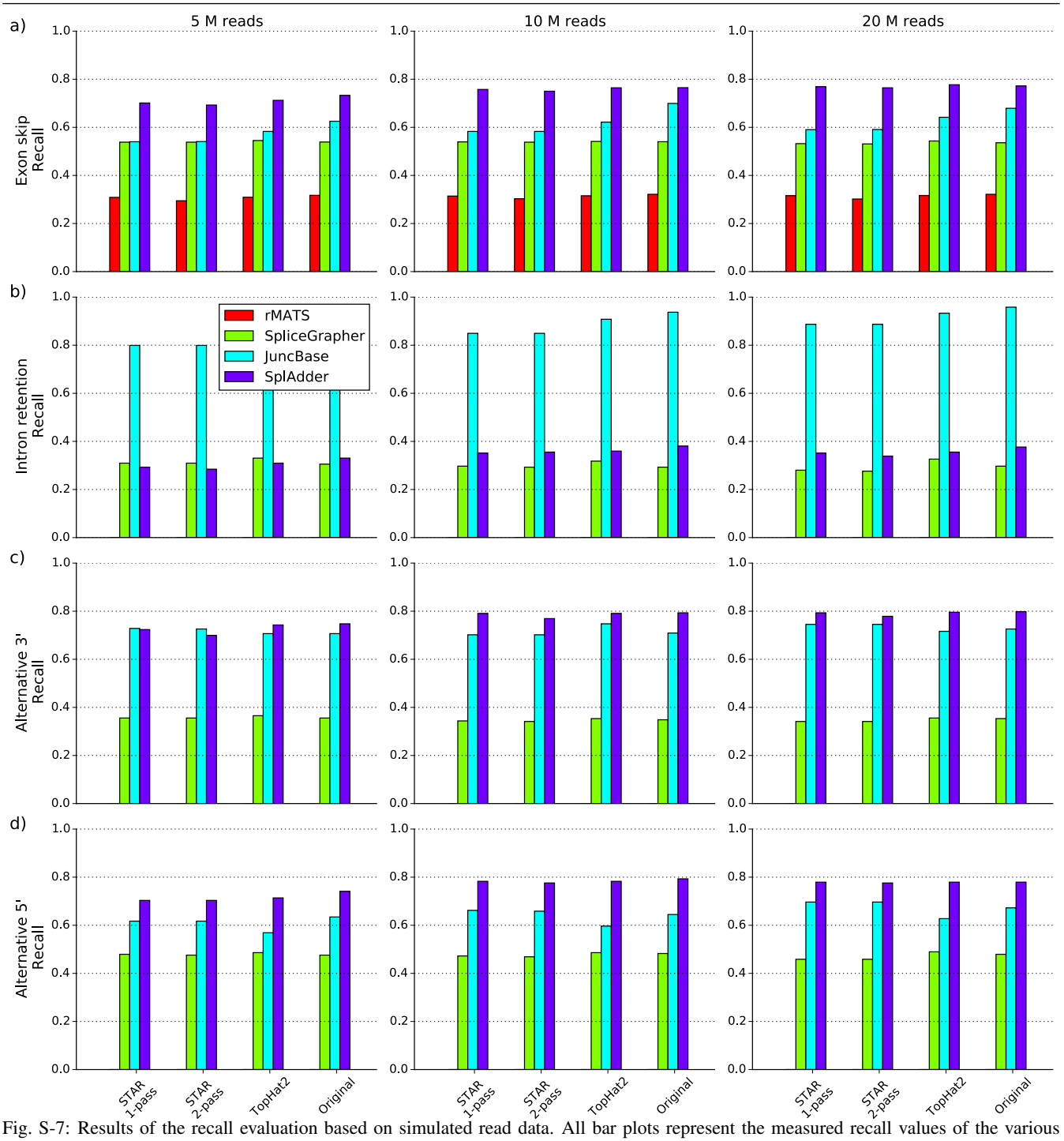

Fig. S-7: Results of the recall evaluation based on simulated read data. All bar plots represent the measured recall values of the various methods compared (*rMATS* (red), *SpliceGrapher* (light green), *JuncBase* (light blue) and *SplAdder* (purple)). Each row represent a different AS event type (from top to bottom: intron retention, exon skip, alternative 3' splice site and alternative 5' splice site) and each column represents a different sample size (from left to right: 5×10^6, 10×10^6, 20×10^6). The groups of bars in the single charts show the different aligners used: (from left to right: *STAR 1-pass*, *STAR 2-pass*, *TopHat*, and the ground truth alignments).

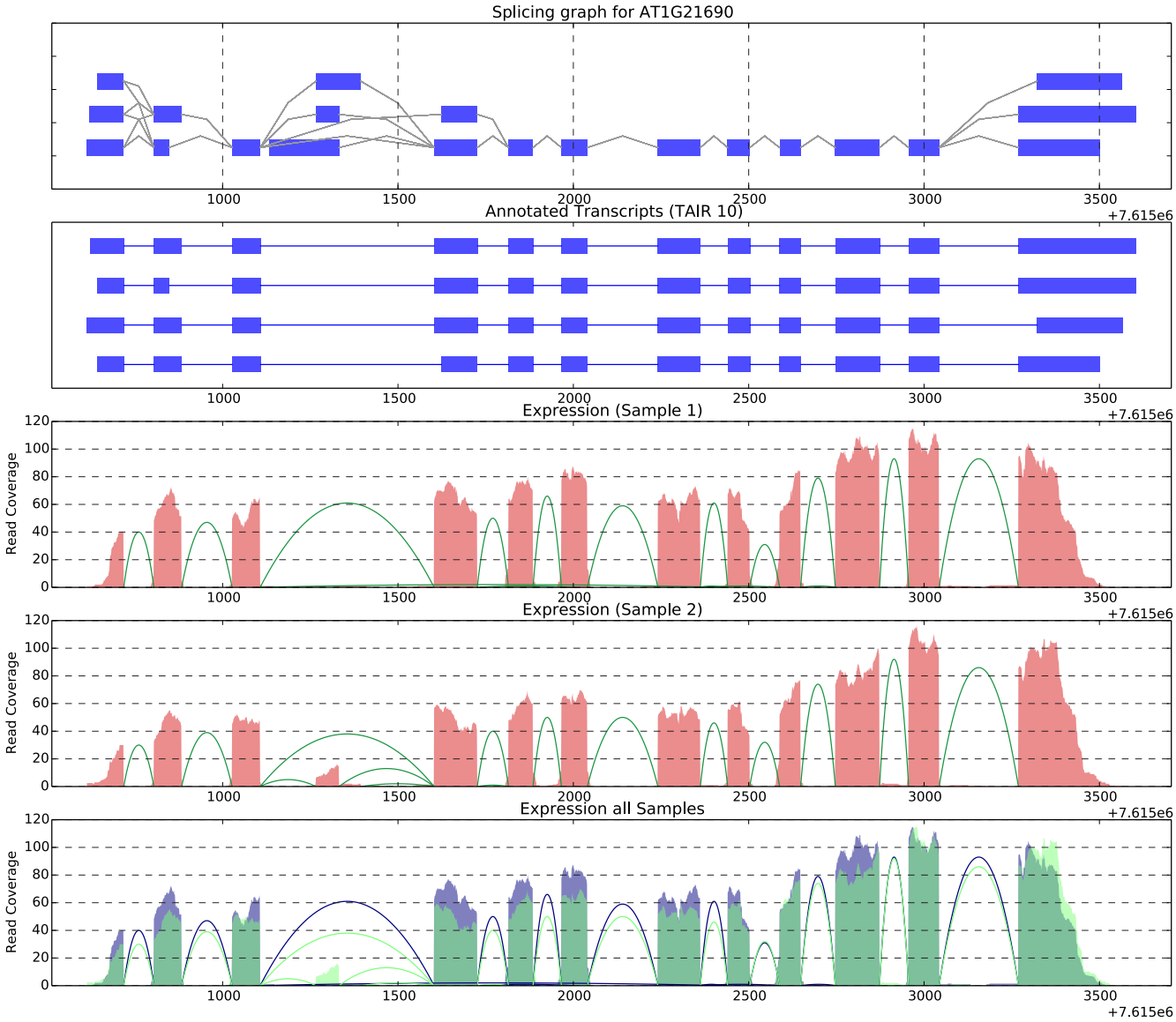

Fig. S-8: Visualization of the splicing pattern occurring at a certain gene locus. The example shows real data taken from experiments on *Arabidopsis thaliana* NMD impaired mutants published in (Drechsel *et al.*, 2013). The upper track shows the splicing graph for the gene AT1G21690 generated by *SplAdder*. The second track shows the annotated transcripts forms available in the TAIR10 annotation. Note, that none of the annotated transcripts contains an additional exon identified by *SplAdder*. When looking at the coverage overview in the WT (Sample 1, track 3) and double-knockdown (Sample 2, track 4) samples, a clear differential usage of that novel exon is apparent. Lastly, track 5 shows both samples in a comparative manner.

Criterion	Value
min exon coverage	5
min fraction of covered positions in exon	0.9
min relative coverage difference to flanking exons	2.05

Table A. Settings for accepted cassette exons

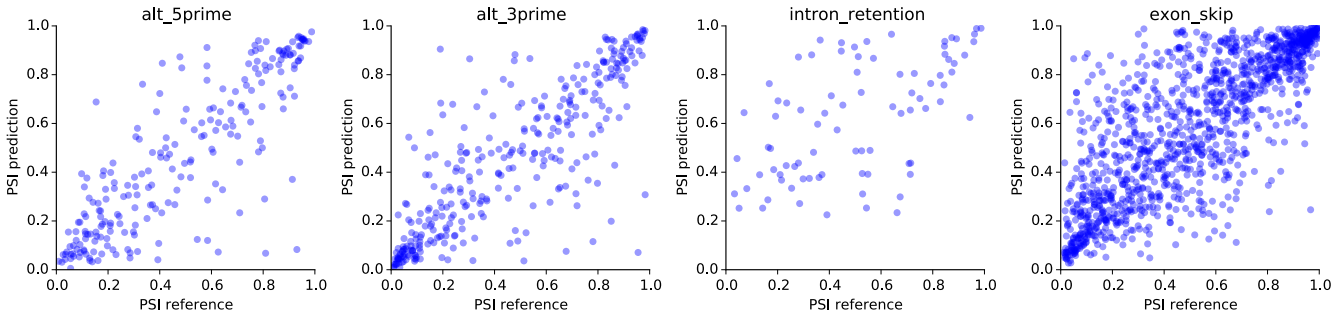

Fig. S-9: Scatter plots of predicted vs. actual PSI values for the *SplAdder* quantifications. Different panels show respective event types (from left to right: alternative 5' splice site, alternative 3' splice site, intron retention and exon skip).

Criterion	**confidence level**			
	0	**1**	**2**	**3**
min intron cov.	1	2	5	10
min fraction of cov. positions in intron	0.75	0.75	0.9	0.9
min intron cov. rel. to flanking exons	0.1	0.1	0.2	0.2
max intron cov. rel. to flanking exons	2	1.2	1.2	1.2

Table B. Settings for accepted intron retentions

Criterion	**Confidence Level**			
	0	**1**	**2**	**3**
min segment length	$\lceil 0.1 \cdot r \rceil$	$\lceil 0.15 \cdot r \rceil$	$\lceil 0.2 \cdot r \rceil$	$\lceil 0.25 \cdot r \rceil$
max mismatches	$\max\{2, \lfloor 0.03 \cdot r \rfloor\}$	$\max\{1, \lfloor 0.02 \cdot r \rfloor\}$	$\max\{1, \lfloor 0.01 \cdot r \rfloor\}$	0
max intron length	350,000	350,000	350,000	350,000
min junction count	1	2	2	2

Table C. Settings for accepted introns, where r stands for the given read length.

Exon Skips	
Criterion	**Value**
min relative coverage difference to flanking exons	0.05
min intron count confirming the skip	3
min intron count confirming the inclusion	3

Multiple Exon Skips	
Criterion	**Value**
min relative coverage difference to flanking exons (avg. on skipped)	0.05
min intron count confirming the skip	3
min average intron count confirming the inclusion	3

Intron Retentions	
Criterion	**Value**
min intron coverage	3
min intron coverage relative to flanking exons	0.05
min fraction of covered positions in the intron	0.75
min intron count confirming the intron	3

Alternative Splice Site Choice	
Criterion	**Value**
min intron count confirming the intron	3
min relative difference of differential exon part to flanking exon	0.05

Mutually Exclusive Exons	
Criterion	**Value**
min relative coverage difference to flanking exons (for exon 1)	0.05
min relative coverage difference to flanking exons (for exon 2)	0.05
min intron count confirming the inclusion (for exon 1)	2
min intron count confirming the inclusion (for exon 2)	2

Table D. Criteria to confirm the different alternative splicing events based on the evidence available in RNA-Seq alignments. Shown are the default values, that can be adapted for fine tuning the confirmation process.

Sample Size	**SplAdder**				**SpliceGrapher**			
	STAR	**STAR-2P**	**TopHat**	**orig**	**STAR**	**STAR-2P**	**TopHat**	**orig**
5M	481	497	415	512	4008	4115	2580	2478
10M	1237	825	700	904	5787	5804	2911	2895
20M	2399	1511	1253	1644	11396	12262	5908	4921
Sample Size	**JuncBase**				**rMATS**			
	STAR	**STAR-2P**	**TopHat**	**orig**	**STAR**	**STAR-2P**	**TopHat**	**orig**
5 M	1182	1168	865	1082	344	344	252	270
10 M	2191	2205	1642	1945	529	521	470	502
20 M	4172	4243	2921	3570	1282	1328	916	954

Table E. Running times for all tools tested on simulated data sets.

Sample Size 5000000					
Method	**Aligner**	**Exon skip**	**Intron retention**	**Alternative 3'**	**Alternative 5'**
rMATS	STAR 1-pass	0.693 (495)	0.000 (0)	0.000 (0)	0.000 (0)
rMATS	STAR 2-pass	0.686 (474)	0.000 (0)	0.000 (0)	0.000 (0)
rMATS	TopHat2	0.688 (497)	0.000 (0)	0.000 (0)	0.000 (0)
rMATS	Original	0.699 (513)	0.000 (0)	0.000 (0)	0.000 (0)
JuncBase	STAR 1-pass	0.700 (882)	0.663 (191)	0.877 (303)	0.851 (179)
JuncBase	STAR 2-pass	0.700 (883)	0.663 (191)	0.875 (302)	0.851 (179)
JuncBase	TopHat2	0.757 (952)	0.677 (210)	0.870 (294)	0.894 (165)
JuncBase	Original	0.763 (1021)	0.678 (215)	0.885 (294)	0.878 (184)
SplAdder	STAR 1-pass	0.792 (1145)	0.573 (70)	0.846 (300)	0.844 (204)
SplAdder	STAR 2-pass	0.791 (1131)	0.598 (68)	0.841 (290)	0.829 (204)
SplAdder	TopHat2	0.792 (1163)	0.624 (74)	0.850 (307)	0.862 (207)
SplAdder	Original	0.793 (1197)	0.586 (79)	0.849 (310)	0.860 (215)
Sample Size 10000000					
Method	**Aligner**	**Exon skip**	**Intron retention**	**Alternative 3'**	**Alternative 5'**
rMATS	STAR 1-pass	0.687 (505)	0.000 (0)	0.000 (0)	0.000 (0)
rMATS	STAR 2-pass	0.676 (483)	0.000 (0)	0.000 (0)	0.000 (0)
rMATS	TopHat2	0.685 (506)	0.000 (0)	0.000 (0)	0.000 (0)
rMATS	Original	0.696 (518)	0.000 (0)	0.000 (0)	0.000 (0)
JuncBase	STAR 1-pass	0.717 (952)	0.661 (203)	0.856 (292)	0.867 (192)
JuncBase	STAR 2-pass	0.718 (952)	0.661 (203)	0.856 (292)	0.867 (191)
JuncBase	TopHat2	0.724 (1015)	0.697 (217)	0.854 (311)	0.867 (173)
JuncBase	Original	0.738 (1142)	0.682 (224)	0.852 (295)	0.875 (187)
SplAdder	STAR 1-pass	0.784 (1237)	0.566 (84)	0.829 (329)	0.839 (226)
SplAdder	STAR 2-pass	0.785 (1225)	0.613 (85)	0.823 (320)	0.829 (224)
SplAdder	TopHat2	0.781 (1248)	0.549 (86)	0.823 (328)	0.840 (226)
SplAdder	Original	0.781 (1249)	0.580 (91)	0.826 (329)	0.839 (229)
Sample Size 20000000					
Method	**Aligner**	**Exon skip**	**Intron retention**	**Alternative 3'**	**Alternative 5'**
rMATS	STAR 1-pass	0.685 (506)	0.000 (0)	0.000 (0)	0.000 (0)
rMATS	STAR 2-pass	0.677 (481)	0.000 (0)	0.000 (0)	0.000 (0)
rMATS	TopHat2	0.688 (509)	0.000 (0)	0.000 (0)	0.000 (0)
rMATS	Original	0.695 (518)	0.000 (0)	0.000 (0)	0.000 (0)
JuncBase	STAR 1-pass	0.710 (964)	0.630 (212)	0.876 (310)	0.869 (202)
JuncBase	STAR 2-pass	0.710 (965)	0.630 (212)	0.876 (310)	0.869 (202)
JuncBase	TopHat2	0.745 (1048)	0.665 (223)	0.871 (298)	0.830 (182)
JuncBase	Original	0.758 (1109)	0.665 (229)	0.879 (302)	0.865 (195)
SplAdder	STAR 1-pass	0.780 (1256)	0.530 (84)	0.857 (329)	0.821 (225)
SplAdder	STAR 2-pass	0.779 (1248)	0.547 (81)	0.855 (323)	0.832 (224)
SplAdder	TopHat2	0.780 (1269)	0.521 (85)	0.842 (331)	0.823 (225)
SplAdder	Original	0.779 (1261)	0.555 (90)	0.843 (332)	0.831 (225)

Table F. Pearson correlation coefficients for predicted vs. true PSI values for different event types and aligners. Values in parentheses are number of events used for correlation. Only events predicted correctly by the respective approach were included for comparison of PSI values. *rMATS* only predicted exon skip events, resulting in values of 0 for the other event types.